Levelset-XFEM Topology Optimization with Applications to Convective Heat Transfer

Peter Coffin

27 August 2014

Contents

Abstract

The goal of this work is to apply levelset eXtended Finite Element Method (XFEM) topology optimization to convective heat transfer problems. The affinity of these problems to develop thin, complicated, and difficult to represent designs drives this work to study the control of these problematic designs through the inclusion of more accurate physical models and solely geometric regularization techniques. Convection is initially considered using a Newton's Law of Cooling (NLC) boundary condition and then via the incorporation of an advection-diffusion temperature field in a fluid governed by the incompressible Navier-Stokes equations. To complete the study, existing and new regularization measures are tested on this work's convective design problems.

Chapter 1

Introduction

The goal of this work is to apply levelset eXtended Finite Element Method (XFEM) topology optimization to coupled convection and structural design problems. As many design problems, such as those studied here, drive towards complicated, finely detailed, otherwise poorly formed designs this work seeks to investigate two fundamental questions to levelset-XFEM topology optimization. First, can introducing more detailed, accurate physical models into the forward analysis deter undesirable designs. Second, what are the best approaches to deterring undesirable designs considering the geometry alone (i.e. the design problem, levelset control). This work will explore the first question by including increasing detailed physics in a heat sink design problem. The second question will be addressed by applying a range of existing and new levelset regularization and control approaches to a heat sink design problem.

1.1 Topology Optimization

Optimization is the process of adjusting parameters of some object in an effort to minimize some characteristic value defined by the object and its parameters. In this work the object to be optimized is the finite element analysis or "forward analysis" whose characteristic value may be a variety one or a combination of values such as a temperature at a particular point or the heat flux through a wall. In a simple parametric analysis, the parameters could be the value of conductivity in a particular material or the height of some feature within the model. In shape optimization the parameters of the analysis are typically some values that define the shape of one or more features within the model. Coefficients to a polynomial defining the surface of a features are one potential set of parameters.

Topology optimization expands the idea of defining the shape of objects in the model to its more general form, that is definition of the topology within the model. The parameters to the forward analysis in a topology optimization problem represent where particular materials and their interfaces lie within the finite element model. The geometric space where the material is to be distributed is referred to as the design domain. In addition to minimizing a particular value, the "objective", one may introduce additional inequality constraints so that particular values may be held within a certain range. For example, a maximum volume of a particular material.

An intermediate set of resultant values from the forward analysis will be called "criteria". These criteria are the set of values from which the objective and constraints will be formed. A simple example would be the desire to minimize both the mass and deflection of a beam, where a simple approach would be to minimize the weighted sum of the mass and the deflection. An additional

constraint may be to limit the maximum stress in the beam. In this case the deflection, mass and maximum stress would be the set of criteria for the problem.

The optimization algorithm is the logic that considers values of the objective and constraints returned from the forward analysis and adjusts the parameters (design variables) until some convergence criteria are met. Due to the substantial number of design variables involved with topology optimization, gradient based optimization algorithms are typically used. Gradients of the objectives and constraints provide the optimizer information about which direction would benefit the objective or result further violation of constraints. So-called "gradient-free" techniques often rely on reconstructing approximate gradients based on forward analysis evaluations, which is particularly costly for computationally expensive problems with large numbers of design variables. The Globally Convergent Method of Moving Asymptotes (GCMMA) of Svanberg (1995) is a common algorithm that is well suited to constrained problems with large numbers of design variables and will be used for this work.

There are two common approaches to incorporate the geometry of a generic material distribution dependent on a vector of continuous variable into a finite element analysis. The first and most common class is that of Solid Isotropic Microstructure with Penalisation (SIMP) or Density methods ((Bendsøe, 1989), (Rozvany et al, 1992)). The second are levelset methods, which will be used for this work. In density methods a ficticious material density is defined at each element. Density values of zero correspond to one material (or void) while values of one correspond to a different material. Intermediate values correspond to some porous-like mixture of the two materials. Levelset methods define a higher order field through the design domain (the levelset field) and define the boundary between two materials as an isocontour of the field. For field values less than zero that region is considered one material, greater than zero the other material and where the field is exactly equal to zero, the boundary between the two.

Levelset methods present a choice of how to incorporate the geometry description into the finite element analysis ((Allaire et al, 2004), (van Dijk et al, 2013)). Ersatz material approaches are similar to density methods, elements fully in one material or the other are treated normally with the material properties of their respective material phase. Elements that lie in more than one phase are treated as a mixture of the two phases, often dependent on the area or volume ratio of the two phases within the element. This work makes use of the eXtended Finite Element Method (XFEM) to incorporate the embedded interface of the levelset method into the finite element analysis. The XFEM was developed to describe cracks in solids and has been applied to a variety of problems with moving interfaces. A recent survey is provided by Fries and Belytschko (2006).

The XFEM relies on adding additional finite element interpolation functions to elements that are intersected by a material interface, referred to as "enriching" the interpolation. This work relies on heaviside enrichment, effectively yielding a set of standard finite element shape functions as associated degrees of freedom for one side of the interface and another set for the opposing side. Heaviside enrichment provides for complete discontinuity of the field at the interface, which while often unnecessary provides a consistent approach for a broad set of physical problems. The XFEM also decomposes the traditional finite element into triangulated (tetrahedra in three dimensions) subdomains upon which the element is integrated. This triangulation also necessarily provides a definition of the interface within the element upon which the interface can be directly integrated.

Levelset methods also vary in how they incorporate the field into the optimization algorithm. Many works directly connect the two by formulating the optimization problem as a solution to the Hamilton-Jacobi equation, which moves the levelset field on each time step. This work defines the levelset field as an explicit function of the design variables, providing for a typical nonlinear programming approach described above. This approach, studied by Wang and Wang (2006), Luo

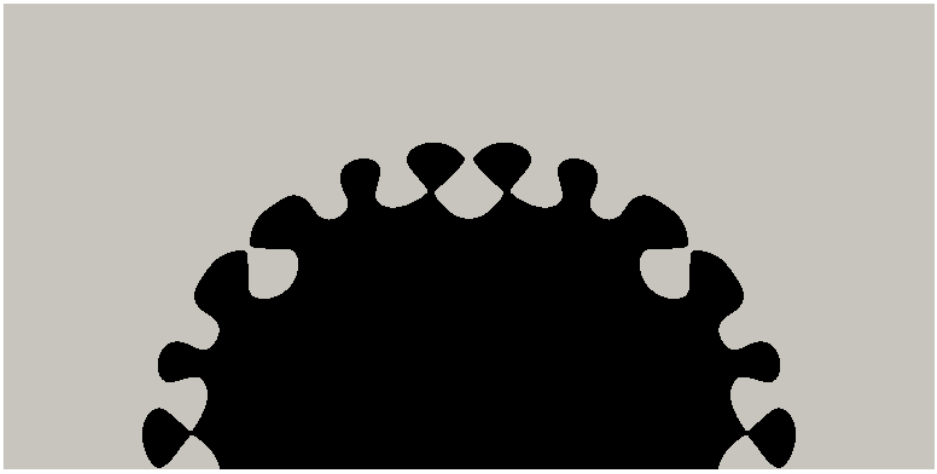

Figure 1.1: Example of thin feature development in Newton's Law of Cooling Convection Problem

et al (2007) and Pingen et al (2010) is often described as the explicit levelset method van Dijk et al (2013). This work defines the levelset field using nodal values of levelset and standard finite element interpolation between them.

The combined optimization and analysis code used for this work is FEMDOC, an in-house, object-oriented C++ code. Distributed vector, sparse matrix and linear solver libraries are provided by the Trilinos package.

1.2 Motivation and Goals

Consider the cooling device design problem from Figure 3.9 (bottom), a two dimensional problem where a heat flux is applied at the center bottom of the design domain. A restricted volume of solid material is allowed to be arranged in the design domain to minimize the temperature at the applied flux. On the in-plane design interface a convective boundary condition is applied using Newton's Law of Cooling (NLC), that is:

$$q = hA(T - T_\infty) \tag{1.1}$$

where q is the flux on some area of the interface, h is the convection coefficient, A the area of the portion of interface, T the temperature of the solid at the interface and T_∞ the far-field fluid temperature. The far-field fluid temperature is approximated as described in Section 3.1 in such a way that fluid inclusions are discouraged. An intermediate design is shown in Figure 1.1. It is clear that the design problem results in fine details that are only limited by the size of the mesh. Small features are beneficial to a number of design problems and have been well described for problems such as structural compliance minimization (Makhija and Maute, 2013).

The difficulty of small features can be broken into two causes, deficiency of the physical model and deficiency of the discretized geometry. In the case of the NLC problem above, it is beneficial to develop many features within a given area. Features close together see no detriment to lying infinitely close to each other, as the flux on the interface only varies with parameters internal to

the feature. As convection is driven by fluid flow at the material interfaces it is clear that as the interface grow closer together there will likely be interference and a detriment to the heat transfer that could actually occur. In this case it would appear that replacing the NLC assumption on the interface with resolved fluid flow and associated heat transfer would alleviate some of the difficulties that arise from features growing close to each other.

Another type of small feature developed in the NLC convection design problem is thinning of the solid features (as opposed to thinning of the regions between the solid features described previous). This behavior is generally governed by the Biot number of the problem, lower numbers yielding thinner features. For low Biot numbers the temperature gradients within the solid material are small. These small gradients mean that regions connecting convective surface area to the applied flux can be very thin before they are detrimental to the problem. These thin regions are physically reasonable as they will be bounded by some optimal size, however there are two issues that arise from them. First, they may be smaller than is reasonable to manufacture without difficulty. Secondly, the optimal width of the small features may be substantially smaller than the levelset discretization can represent. Inconsistent representation of the geometry can lead to poor convergence of the design as the optimization algorithm effectively encounters discontinuities in the criteria-design variable relationship. A more detailed discussion of the behavior of this problem is provided in Section 3.1. A detailed discussion of representation of small features by the levelest will be provided in Section 2.1.

This work will study and attempt to alleviate poor behavior in convective heat transfer problems in two ways, by incorporating more detailed physical models and by incorporating measures and techniques that work on the geometric design alone. The incorporation of more detailed physical models will be provided in the applications section. The applications section contains two paper drafts to be submitted for publication and one for future work. The first paper studies the most simple convection problem, modeling the solid material alone with varying applications of the NLC flux to the design interface. The second paper studies a natural convection problem incorporating an incompressible Navier-Stokes fluid model with the advection-diffusion defined temperature field. The final paper for which work is to be performed considers a heat exchanger/cooling device design problem incorporating incompressible Navier-Stokes fluids, an advection-diffusion temperature field and a linear elastic structure with thermal expansion.

Discussion of the control of geometry alone will be provided in Chapter 2 and will be applied to the design problems of Chapter 3. This work will consider two approaches to providing levelset geometry control, regularization measures (element local and global) and robust optimization techniques, all described in Section 2.2.

Chapter 2

Levelset Control for Topology Optimization of Heat Transfer Problems

To produce meaningful and manufacturable designs it is often necessary to identify and discourage features below a particular size, due to manufacturing or discretization limitations. In this work geometry is defined by the zero isocontour of a levelset field discretized by standard bi and tri-linear finite element shape functions. As a result, representing geometry features smaller than the finite elements may yield undesirable artifacts of the levelset discretization. In Section 2.1 this work the details of particular problems associated with discretization artifacts will be discussed. A discussion of regularization approaches to be investigated will be shown in Section 2.2. Results of application of regularization approaches will be shown in Section 2.3 as well as in the associated application works of Chapter 3.

2.1 Difficulties due to discretization issues

In an effort to characterize commonly observed behaviors associated with small features in finite element discretized levelsets we will consider the optimization problem in Figure 2.1. The goal of the optimization is to arrange material 1 in the domain to minimize the temperature at point B within some volume constraint on material 1. A heat flux (into the domain) is applied at point B while a fixed temperature is placed at two points (A) at the top of the domain. The diffusivity of material 1 is 10 times that of material 2. The expected final design is a simple v-shape connecting points A to B, the thickness of the V depending on the volume constraint. Lowering the volume constraint and starting the optimization from a thick v-shape allows for the development of thin features of a desired size.

2.1.1 Final (Optimized) Geometry

The goal of any optimization is to produce a final design that minimizes the objective value within the given constraints. Visually identifiable artifacts of the levelset discretization in the final design are obvious signs that the design features are being limited or poorly represented by the discretization. The final design including artifacts is some mixture of the actual best solution and that which can be described using the chosen discretization. In the best case the designs are only slightly shifted in the orientation of geometric features, however more substantial differences may result.

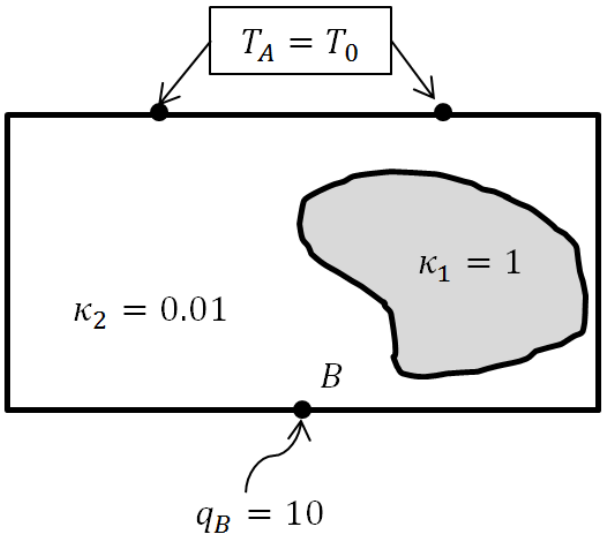

Figure 2.1: Example heat transfer design problem for exhibiting small features

A commonly visible discretization artifact in designs represented with the finite element interpolation used here is the alignment of small features with element edges. Considering the two-dimensional discretization, the levelset field is represented using bi-linear finite element interpolation of nodally defined values. This discretization means that there is a limited set of intersection patterns that can be developed on any particular element, shown in Figure 2.2.

Features that are thinner than the width of an element are limited to two basic configurations, substantially limiting their geometric orientation. Features must either follow element edges or lie diagonally across elements. Considering a patch of four elements the three basic configurations are shown in Figure 2.3: one (a) where the feature falls diagonally across the elements making a set of double intersections, one (b) that makes single intersections on neighboring elements following element edges and a combination of the two approaches (c).

An example of the preference of features to follow these orientations is shown in Figure 2.4. In Figure 2.4 the feature is a thin connection of highly conductive material attempting to run along a line approximately 30 degrees from vertical. The overall connection ends up with a stair-step shape across the domain. As the reader may already anticipate, having strong preference of small feature orientation can result in non-smooth relations between design variables and the optimization criteria. These behaviors will be discussed in the next section.

2.1.2 Objective and Constraint Smoothness through Intermediate Designs

Discontinuities or jumps in the optimization criteria and their derivatives with respect to the design variables (nodal levelset values) can have deleterious effects on the smooth convergence of the objective. A common behavior faced during optimization is sharp discontinuity in criteria when connections between a particular phase are made or deleted. Considering a typical solid mechanics, thermal or fluid problem with a void second phase it is obvious how there will necessarily be a jump in the state dependent criteria when features are connected or disconnected. When considering two non-void materials it could be argued that with fine enough resolution there should be a smooth

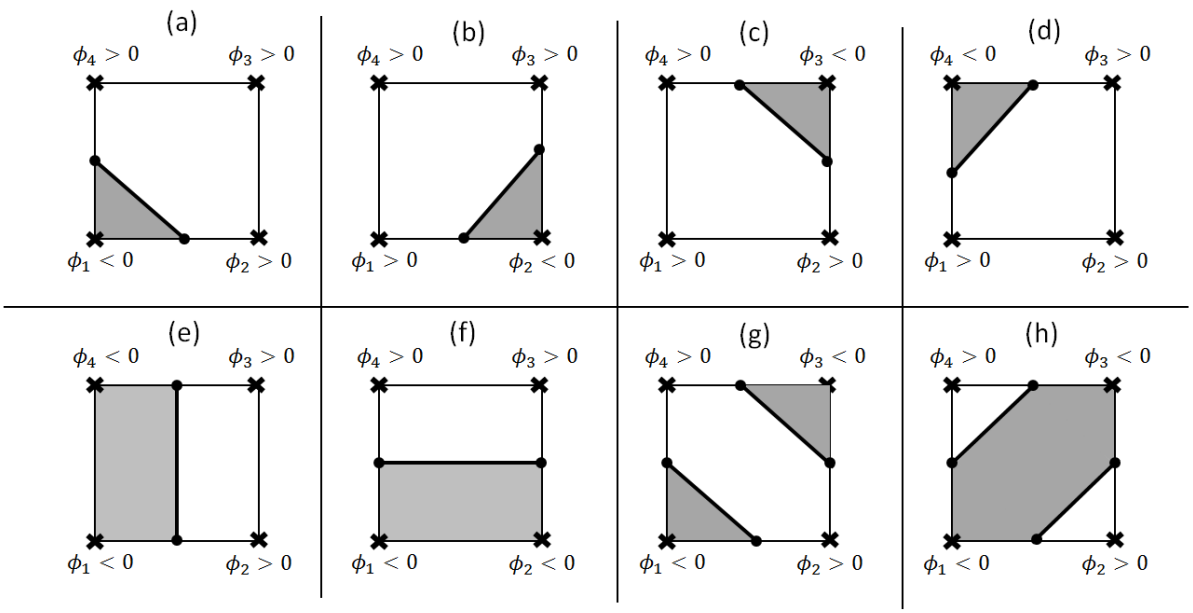

Figure 2.2: Examples of possible intersection configurations using bi-linear finite element interpolation

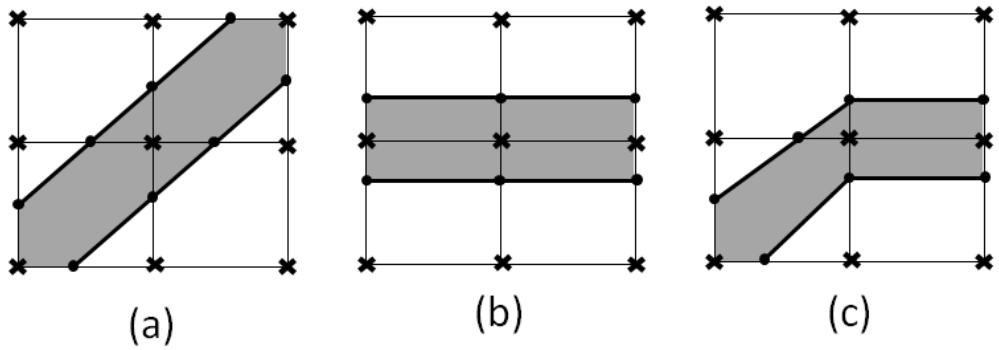

Figure 2.3: Examples of possible intersection configurations for sub-grid features

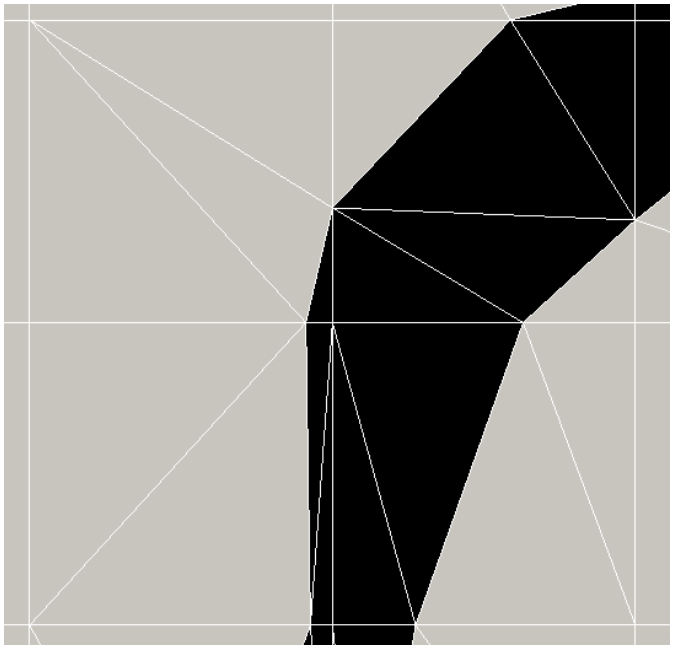

Figure 2.4: Example of thin geometric feature aligning with intersection patterns

change as two features meet. Unfortunately for typical problems (with an order of magnitude or more difference between material parameters) the step size during design iteration needed to resolve the jump is small compared to the typical optimization step size.

Considering the extreme case of material-void problems, the two configurations, connected and unconnected, represent two substantially different geometries that have very similar levelset fields. The issue is particularly difficult because sensitivity information in either configuration does not indicate the nearby jump in criteria corresponding to the other configuration. This leads to the optimizer stepping through connections or disconnections inadvertently. In the case of material-void there is no gradient information leading the optimizer to rejoin disconnected material features. Inability to rejoin is poor behavior if the connected configuration yielded a better objective value. In more benign material-material problems such as those of 3.1.4 oscillatory behavior can be experienced as the optimizer steps back and forth connecting and disconnecting the features.

The scenarios described above ignore the important compounding problem of resolving the small connections well. As described in Section 2.1.1 the finite element discretization of the levelset field is only able to describe thin features crossing elements in particular orientations. Thin features crossing along diagonals are particularly problematic as on an element the layout of phases contains uncertainty.

Consider 2.2(g) and (h), for both configurations the signs of the nodal levelset values are the same. For this work the phase of the center region is determined by interpolating the levelset value to the center. If the nodal levelset are approximately equal in magnitude around the element the phase of the center region can be switched with a small change in nodal levelset value. Consider the nodal values of ($[\phi_1, \phi_2, \phi_3, \phi_4] = [-1, 1, -1, 1]$) that yield an interpolated value at the center of zero. Perturbing $\phi_1 = \phi_1 + \epsilon$ (where $\epsilon > 0$) would yield Figure 2.2(g) while perturbing $\phi_1 = \phi_1 - \epsilon$ would yield configuration (h). In this example for small perturbations of nodal levelset value the discretization effectively closes or opens a geometric gap of $\frac{\sqrt{2}}{2}h$, where h is the element width.

2.2 Levelset Control Approaches

This work will consider three primary categories of levelset control measures, locally computed regularization measures, global regularization measures and robust optimization inspired techniques. Locally and globally computed regularization measures will be categorized as approaches where a measure can be computed from the design and simply used to augment the objective function as a penalty factor or be added as a constraint. Robust optimization techniques will consider methods where an uncertain field of design perturbations may be included in the optimization problem or simply an additional set of worst-case scenario designs as in (Sigmund, 2009) and (Jang et al, 2012).

2.2.1 Element Local Measures

One ideal characteristic of a measure is locality, i.e. it can be computed at any given point based only on information about an area within a small radius of the point. This section will be restricted to measures that can be computed and integrated element-by-element. This restriction allows one to incorporate the measure into typical domain decomposition approaches used in finite element analysis without the need to communicate extra information. A short overview of common measures will be first provided in Section 2.2.1 and then a new gradient based measure will be proposed in Section 2.2.1 and applied in Section 3.1.

Perimeter, Overall Gradient and Intermediate Values The first and simplest locally computed measure is perimeter, which can be written as:

$$P = \int d\Gamma \tag{2.1}$$

where Γ is the material interface. It has been noted in a number of works ((Maute et al, 2011), (van Dijk et al, 2012)) that this can be used to well regularize the optimization problem. It is particularly convenient for levelset-XFEM approaches as the XFEM provides for direct integration along the interface. However the perimeter is not directly a measure of small features. While perimeter regularization may discourage designs that contain small features it may also discourage otherwise good designs that simply have large perimeter. It was found in Section 3.1 that perimeter regularization could not fully eliminate certain forms of undesirable features.

Two related measures are Tikhonov regularization and penalization of intermediate levelset values. Tikhonov regularization penalizes the magnitude of levelset gradient as:

$$\Pi = \int ||\nabla \phi|| d\Omega \tag{2.2}$$

where ϕ is the levelset value and Ω the entire domain. Considering a situation, where nodal levelset values are limited to either $+1$ or -1, this measure behaves similarly to a perimeter penalization. In actual application, this method both limits perimeter and encourages shallow levelset fields near the interface. Penalization of intermediate levelset values can be performed by a variety of measures as used by Luo et al (2009), Wang and Zhou (2004) and Mohamadian and Shojaee (2011). Conversely to Tikhonov regularization, penalization of intermediate values will yield steep levelset fields at the interface. As described by Burger and Osher (2005) and van Dijk et al (2012) particularly flat or steep levelset fields at the interface will yield poorly scaled sensitivities.

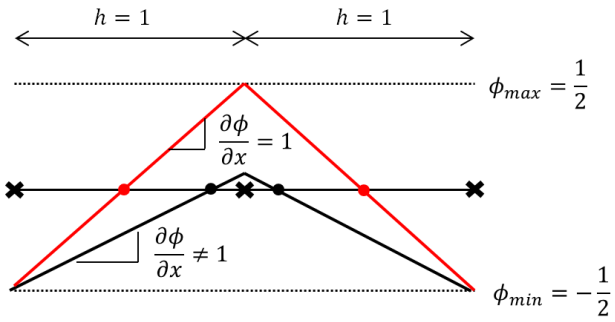

Figure 2.5: Demonstration of how gradient measure of Eqn 3.6 identifies small features with appropriate levelset value bounds, small feature with unsatisfied levelset gradient in black, satisfied levelset gradient in red

New Gradient Measure In Section 3.1.2 a new measure inspired by maintaining well scaled sensitivities at the interface is proposed. Defined in Equation 3.6 the measure contains two terms, one $((|\nabla\phi| - \phi_p)^2)$ indicating a difference from the desired levelset slope value of ϕ_p and one limiting the measure to regions near the zero levelset isocontour ($e^{-\phi^2 e_p^2}$). Careful application to design problems has shown that in addition to simply maintaining well-scaled sensitivities, sub-grid features can be identified and deterred.

In Figure 2.5 two levelset fields are shown for a one-dimensional problem. Given the bounds on the levelset field (chosen as half the element width), the smallest feature can be created by setting the left and right nodal values to $-\frac{1}{2}$ and the middle node to a small positive value, shown by the black line. This levelset field will vary from the prescribed slope $\phi_p = 1$ however and as such, the gradient measure of Eqn. 3.6 will return a nonzero value. The red line shows the smallest feature that would satisfy the prescribed slope, being one element width in length.

2.2.2 Global Measures

An important limitation to locally computed measures is that they can only make use of information within their region of locality, in this case the finite element. Therefore we consider locally computed measures to generally only be capable of detecting sub-grid features, those smaller than an element. We will consider global measures to include those that require the solution to an additional Partial Differential Equation (PDE) or information from local patches larger than one element. The patch size for which information is required is often related to the size of the largest features of interest, so even the global measures here may be effectively local.

Guo et al (2014) make use of a sign-distance function levelset to compute medial surfaces of the design geometry. Integrating a measure:

$$g_1 = \int \left[max\left(0, \left[d - \phi^{SDF}\right]\right)\right]^2 d\Gamma_{MS} \tag{2.3}$$

where d is the prescribed minimum feature length and Γ_{MS} the medial surface. The sign-distance function is necessary in two ways, in identifying the medial surface (finding ridges in the levelset field) and in identifying the distance to nearby material interfaces at any point on the medial surface. To apply this (or similar) approaches to our explicit levelset representation an additional levelset field could be computed for the purpose of feature size measurement.

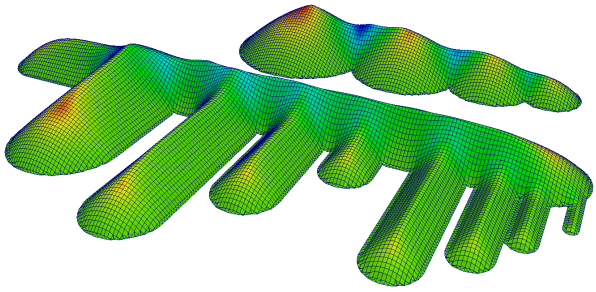

Figure 2.6: Reconstruction of approximate sign distance function using solution to poisson equation

Figure 2.6 shows a sign-stance-like field reconstructed by solving the Poisson equation. The equation is computed as:

$$\nabla L = q_n \tag{2.4}$$

where q_n represents the desired slope of the field. The field value at the material interface is prescribed to zero using stabilized Lagrange multipliers. The approximate value of levelset can be computed as:

$$\tilde{\phi}^{SDF} = -\left(\left|\frac{\partial L}{\partial x}\right| + \left|\frac{\partial L}{\partial y}\right|\right) + \sqrt{\left(\left|\frac{\partial L}{\partial x}\right| + \left|\frac{\partial L}{\partial y}\right|\right)^2 + 2L} \tag{2.5}$$

as described by Tucker (1998). A variety of wall-distance reconstruction methods have been developed for the purpose of wall-distance dependent turbulence functions or boundary layer meshing ((Jones et al, 2006), (Tucker, 2003)).

A new global measure computed based on an approximated sign-distance field is presented here. Computed at a given point $\mathbf{x}_i$ on the material interface this new global measure is:

$$m_i = \left(\int w_i(\mathbf{x})\, H\left[\mathbf{n}_i \cdot \nabla \phi^{SDF}\right] d\Omega\right) / \left(\int w_i(\mathbf{x})\, d\Omega\right) \tag{2.6}$$

where $\mathbf{n}_i$ is the interface normal at point $\mathbf{x}_i$, $H[a]$ a smoothed Heaviside function (Equation 3.13) and $w_i(\mathbf{x})$ a weighting function computed as:

$$w_i(\mathbf{x}) = max\left(0, \mathbf{n}_i \cdot \left[\frac{\mathbf{x} - \mathbf{x}_i}{|\mathbf{x} - \mathbf{x}_i|}\right]\right) \cdot H\left(r - |\mathbf{x} - \mathbf{x}_i|\right) \tag{2.7}$$

defined for a spatial coordinate $\mathbf{x}$ relative to interface point $\mathbf{x}_i$, with a filter radius r where $H(a)$ is the Heaviside function of Equation 3.30. The mean value over the interface is computed as:

$$M = \left[\int m_i d\Gamma_{1,2}\right] / \left[\int d\Gamma_{1,2}\right] \tag{2.8}$$

where $\Gamma_{1,2}$ is the design interface. Within some chose radius of the interface, the direction of the interface normal is compared to the gradient of the estimated sign distance (SDF) field 2.5. If the dot product of the interface normal and SDF is negative the contribution is zero as the SDF is growing away from the interface. Conversely, a positive value indicates that the SDF is decreasing away from the interface, indicating that the SDF is being driven by another opposing section of

interface. To detect features of width w the filter radius should be set such that $r = \frac{w}{2}$. The weight w_i restricts the area of interest to those with the radius r of the point on the interface and to those in the direction of interface normal.

Chen et al (2008) have investigated the use of another globally computed measure, referred to as a quadratic energy. This measure consists of a double integral over the material interface. The value being integrated compares the distance between the two integration points on the interface as well as the different in interface orientation. Effectively the measure detects interfaces near each other with differing orientation.

2.2.3 Robust Design Techniques

Robust optimization approaches work to control the levelset field and small features by considering the uncertainty in material, loading or geometric parameters. Chen and Chen (2011) consider the complete robust problem, incorporating a random normal velocity field on the levelset interface using Karhunen-Loeve expansion. A simpler approach applied to density methods by Sigmund (2009) considers only a subset of 'worst-case' designs. In the density approach this consists of either perturbing all values of density in the domain or projecting the density field at varying values. This effectively thickens or thins regions depending on the direction of the perturbation. Jang et al (2012) have taken this approach and applied it to levelset topology optimization using an implicit levelset representation. This simple approach is an interesting way to incorporate uncertainty and limitation of certain feature sizes in our optimization and is an area for future work.

2.3 Preliminary Results

2.3.1 Element Local Measures

Figure 2.7 shows a comparison the influence of a selection of regularization parameters. The baseline design is a relaxed, penalized void NLC optimization problem. In design (b) the perimeter penalty coefficient is increased by a factor of ten, substantially changing the final design. The increase of the perimeter penalty leads to a thicker design with fewer structures.

Figure 2.7 (c) increases the gradient measure (Equation 3.6) penalty coefficient by a factor of 1000. While the number of features and their thickness is maintained the orientation of the features is noticeably different. It appears that the additional gradient measure penalty is yielding slightly thicker features along their entire length, leading to the feature tips exhibiting less mesh dependency.

The final design (d) in Figure 2.7 depicts the influence of an increased smoothing radius. The radius is increased from 2.4 times the element width to 3.6 times the element width, effectively including an extra set of nodes within the smoothing radius. The difference in the final design is visually substantial, yielding fewer, thicker features. The features also appear to have substantial mesh dependent artifacts at their tip that are not as well defined in the other designs. The exact cause of these more defined artifacts is unknown.

As discussed in Section 3.1.4 the effective application of these measures is sometimes not straight forward for difficult problems. Penalties on the gradient measure or perimeter can be applied and scaled based on the initial design such that their contribution is approximately a factor of ten or one hundred less than the value to be minimized. For relatively well-formed problems this approach

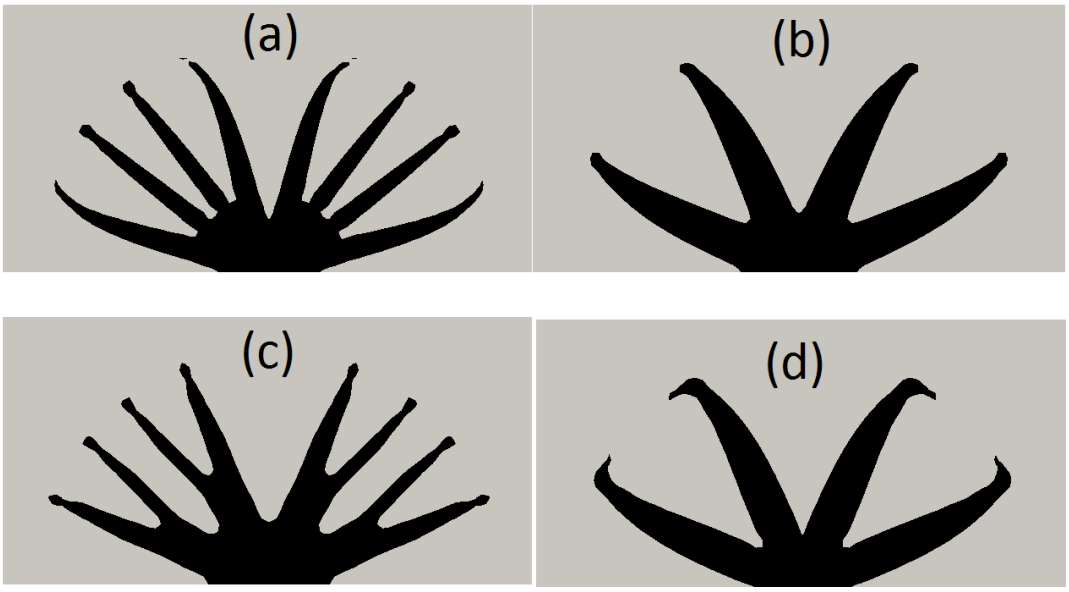

Figure 2.7: Comparison of regularization penalty influences, (a) baseline (bottom design from Figure 3.14), (b) factor ten larger perimeter penalty, (c) factor 1000 larger gradient measure penalty, and (d) 1.5 larger smoothing radius

works well, as shown in Figure 2.7. For particularly difficult problems, such as the well-resolved NLC convection problem of Section 3.1.4 it can be necessary to introduce constraints on the gradient measure and perimeter. The values to constrain these measures at has been determined by noting the values at designs just prior to undesirable features being developed. Even with this prior knowledge it may still be necessary to further limit (lower the constrained value) the measure to produce well-formed designs.

2.3.2 Global Measures

Preliminary work has been completed to validate the concept of the measure described in Equation 2.6. The measure was able to well identify small features and differentiate length differences between example features. Figure 2.8 shows the absolute difference between the actual wall-distance d and the wall distance computed $\tilde{\phi}^{SDF}$ via Equation 2.5. This means that positive values of difference indication an overestimate of distance to the wall by Equation 2.5 and negative values an underestimate. Figure 2.8 shows that in typically for convex features (tips of features) the measure provides a slight overestimate of the distance and an underestimate of the distance when considering concave features (where features meet a body).

To understand the behavior of the measure in Equation 2.8 we close a gap as shown in Figure 2.9. The entire design interface is representing a gap that runs across the center of the domain. Varying the size of this gap and plotting the resulting value of Equation 2.8 for varying radius r. As expected, as the half-width of the gap meets the filter radius of the measure the measure increases in value, detecting the small feature. Once the gap closes beyond a certain point the measure no longer increases in value as the integration of the region in Equation 2.6 (with nonzero weight) is no longer well represented discretely.

To evaluate the influence small features (relative to the overall interface length) on the proposed

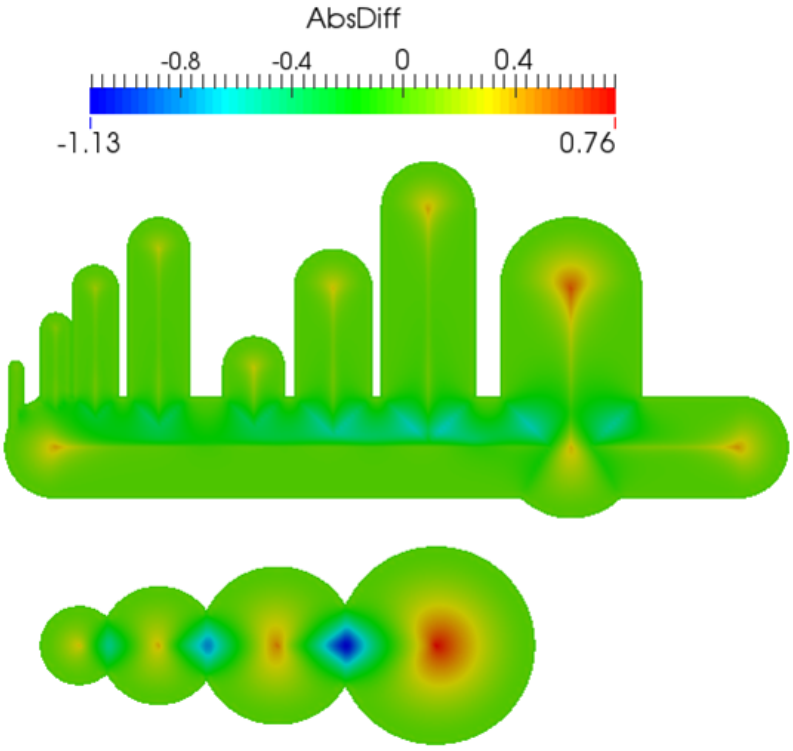

Figure 2.8: Absolute difference between actual and estimated sign-distance functions, maximum true sign-distance value in mesh: 2.5

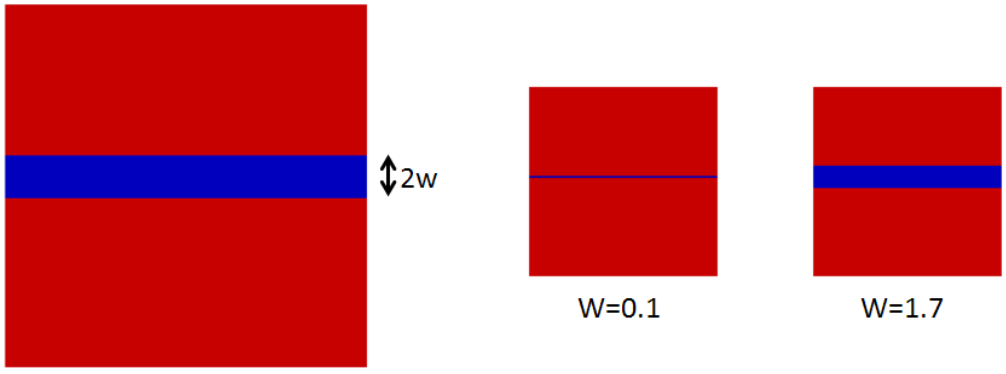

Figure 2.9: Problem setup (and two example gap sizes) for test of feature size detection measure (Equation 2.8)

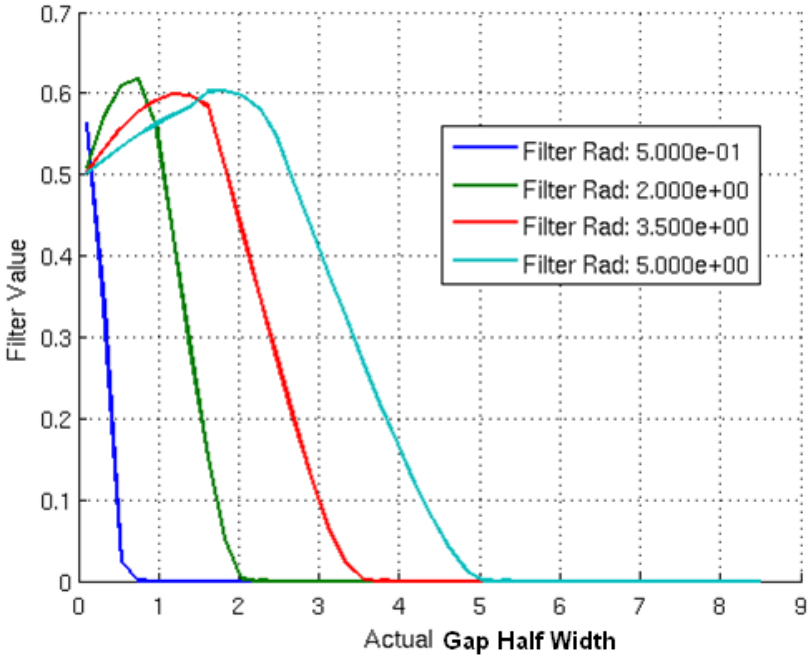

Figure 2.10: Variation of detection measure value for varying gap width and varying filter radius, levelset configuration in Figure 2.9

measure a second problem setup is presented in Figure 2.11. Figure 2.12 shows a plot of measure value with varying gap width. The behavior is similar to that of Figure 2.10 however the magnitude of the jump is substantially smaller, expected considering the plotted measure is computed as a mean value of the measure over the interface.

Finally a levelset field is defined with series of semi-circles in Figure 2.13 to verify that the measure behaves well for curved interfaces. Figure 2.14 shows that the measure continues to behave as expected. The proper machinery for the sensitivity analysis of the measure with respect to the design variables has currently not been completed. The non-local form of the measure and its direct and indirect (through state variables) dependence on the design variables lead to a somewhat complicated implementation.

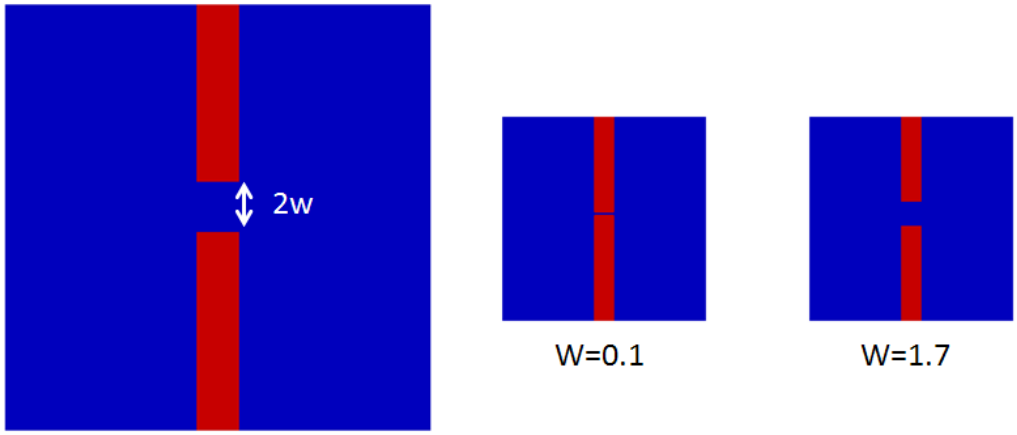

Figure 2.11: Problem setup (and two example gap sizes) for second test of feature size detection measure (Equation 2.8)

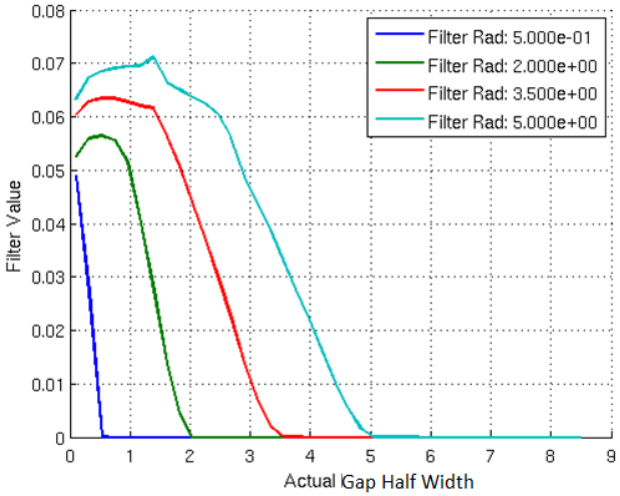

Figure 2.12: Variation of detection measure value for varying gap width and varying filter radius, levelset configuration in Figure 2.11

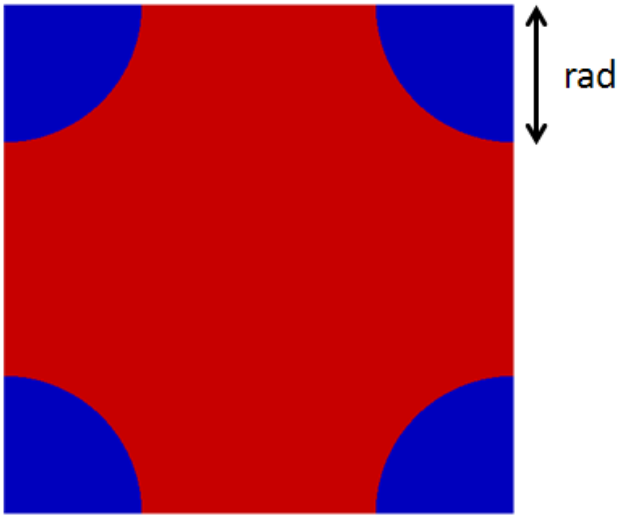

Figure 2.13: Problem setup for third test of feature size detection measure (Equation 2.8)

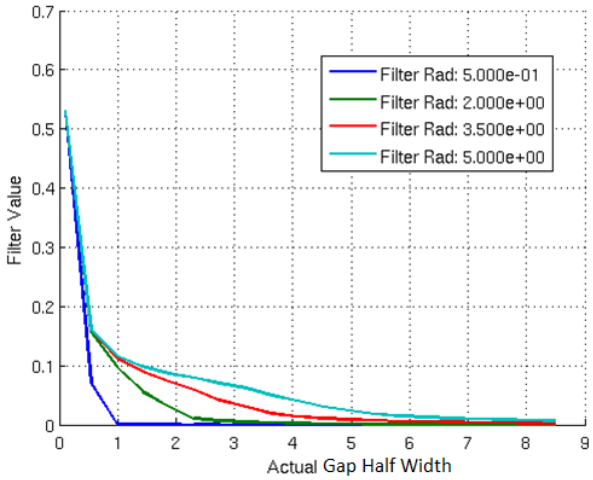

Figure 2.14: Variation of detection measure value for varying gap width and varying filter radius, levelset configuration in Figure 2.13

Chapter 3

Applications

3.1 Topology Optimization of Convection Problems with Newton's Law of Cooling

3.1.1 Introduction

Convection is the process of heat transfer as a result of the motion of fluids. This process is used for thermal management in many devices, such as cooling of processors in consumer electronics or automobile disc brakes. Particularly in electronics, as overall device size shrinks, the development of space efficient cooling mechanisms becomes increasingly important. This requires optimal geometries of the cooling modules to enhance the energy transport across material interfaces. This work will investigate the use of topology optimization to design convective cooling devices.

Convection is typically divided into two categories: natural convection, where the temperature dependent buoyancy forces drive the fluid flow, and forced convection, where an external force drives the flow. Matsumori et al (2013), Yoon (2010), Lee (2012), McConnell and Pingen (2012), Marck et al (2013), Koga et al (2013), Makhija and Maute (2014) have studied topology optimization of forced convection problems, resolving flow and temperature fields. Fully-coupled natural convection problems have seen substantially less attention and to date has been studied only by Alexandersen et al (2013).

In the studies above, the flow is predicted by the incompressible Navier-Stokes or the hydrodynamic Boltzmann transport equations and the thermal energy transport is described by an advection-diffusion model. While this approach accurately captures the relevant physical phenomena in the fluid, it comes with a large computational cost. To bypass this issue, a common engineering approach to approximate the convective heat flux by applying a temperature dependent heat flux on the fluid-solid interface. Thus, the flow field is not directly resolved and the computational cost is reduced. The flux boundary condition, referred to as Newton's Law of Cooling (NLC), is defined as:

$$q = \int_{\Gamma_{FS}} h\left(T - T_\infty\right)\ d\Gamma, \tag{3.1}$$

where q is the flux, h the convection coefficient, T the temperature at the fluid-solid interface, Γ_{FS}, and T_∞ the ambient fluid temperature. The value of convection coefficient, h, is dependent on the interface geometry, fluid motion, and fluid material properties (Cengel et al, 1998). In this study we model the convective flux, q, by NLC with a constant convection coefficient, limiting the work to problems where fluid flow at the fluid-solid interface is insensitive to the design.

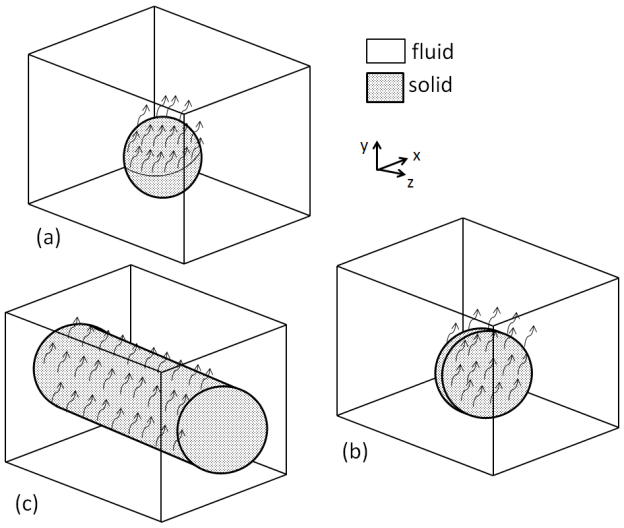

Figure 3.1: General three dimensional (a) convection problem and two dimensional simplifications (Thin (b), Thick (c))

For integrating the NLC model into topology optimization it is convenient to distinguish between the following geometric configurations. Consider a three dimensional solid body immersed in a fluid, as shown in Figure 3.1(a). The body convects heat at the fluid-solid interface that is marked in gray. This general three dimensional configuration can be simplified to a two dimensional problem by considering either a thin or thick body. In both cases the design domain is assumed to be in the x-y plane. In Figure 3.1(b) a thin body is depicted that convects heat primarily at two surfaces with normals in the z-direction, i.e. normal to the design domain. Convection at the remaining surface, whose normal is in the x-y plane is negligible and therefore ignored. A thick body is shown in Figure 3.1(c). Here the surfaces with a normal in the x-y plane convect heat. The convection on surfaces with normals orthogonal to the design domain may or may not be considered.

The majority of topology optimization methods considering heat convection via NLC are based on the density or SIMP (Solid Isotropic Microstructure with Penalisation) approach, which was originally developed by Bendsøe (1989) and Rozvany et al (1992) for structural topology optimization. The geometry of the body is described by its material distribution within the design domain. A fictitious porous material is introduced to allow for the continuous transition between "void" and solid material, i.e. $\rho = 0$ and $\rho = 1$. The material properties are interpolated as functions of the density. For an introduction to density methods, the reader is referred to (Bendsøe and Sigmund, 2003); (Sigmund and Maute, 2013) review recent developments.

The NLC model has been integrated into a SIMP topology optimization methods considering the thin 2-D configuration, for example, by Bruns (2007), Sigmund (2001b), Yin and Ananthasuresh (2002), Seo (2009), and Alexandersen et al (2013). For this configuration, the NLC model can be conveniently embedded into density topology methods as the convection coefficient can be interpolated as function of the density, similarly to the material properties. For example, setting the convection coefficient to zero in the void phase the integration of the heat flux over the entire design domain is equivalent to integrating the heat flux over just the solid domain.

Considering the thick 2-D or the general 3-D configurations in density topology optimization methods is more challenging as for these configurations the geometry of the fluid-solid interface

is not explicitly defined via the material distribution. To approximate the location of the fluid-structure interface and to apply a convective heat flux, Yin and Ananthasuresh (2002) and Iga et al (2009) interpolate the convection coefficient such that the convection coefficient is maximum for an intermediate density value and vanishes at extreme density values, i.e. $\rho = 0$ and $\rho = 1$. Alexandersen et al (2013) follow the method suggested in Bruns (2007) and approximate the location of the interface via the spatial gradients of the density distribution; the convection coefficient is defined as a function of the density difference between neighboring element. As similar approach is adopted by Yoon and Kim (2005) using the element connectivity parameterization method. Moon et al (2004) approximate the convective flux by surrounding the solid with a fictitious fluid phase of low diffusivity at ambient temperature.

Level set methods provide an interesting alternative to density topology optimization methods, in particular for problems with heat convection. The fluid-solid interface is defined explicitly via the iso-contour of the level set function, ϕ at a given value, typically $\phi = 0$. The reader is referred to (van Dijk et al, 2013) for an introduction and a review of recent development of level set methods. Yamada et al (2011) apply a level set method to thick 2-D convection problem. The design is advanced in the optimization process via the solution of the Hamilton-Jacobi equation and an Ersatz material approach is used to project the geometry onto the finite element heat transport model. Following the approach of Osher and Fedkiw (2002), the convection coefficient is defined as a function of the level set function and its spatial gradient, such that convection is confined to the vicinity of the fluid-solid interface.

The Ersatz material approach requires the interpolation of physical properties as functions of the level set function. Similarly to density methods, this may lead to the formation of geometric artifacts and smears interface phenomena, affecting the resolution and accuracy of the finite element predictions (van Dijk et al, 2013). To overcome these issues, we introduce and study in this work the eXtended Finite Element Method (XFEM) for level set topology optimization of heat transport problems subject to surface convection modeled by NLC. The XFEM allows one to approximate the state variables and to integrate the weak form of the governing equations such that the geometry of material interfaces is accurately captured. The XFEM was originally developed to describe the propagation of cracks in solids and later applied to a broad range of problems with moving interfaces. The reader is referred to Fries and Belytschko (2006) for a recent survey of the XFEM. In the context of topology optimization, the XFEM bypasses the need for material interpolation schemes and does not smear interface phenomena. These features are particular promising for convection problems as the NLC flux can be integrated along the immersed fluid-solid boundary. We will compare the resolution and accuracy of the XFEM formulation of NLC against SIMP and Ersatz material approaches used in previous studies.

In this work, we embed the XFEM into an explicit formulation of the level set method where the parameters of the discretized level set functions are defined as explicit functions of the optimization variables and the parameter optimization problem is solved by nonlinear programming methods. This approach is often referred to as the explicit level set method van Dijk et al (2013) and has been studied, for example, by Wang and Wang (2006), Luo et al (2007), and Pingen et al (2010). The specific approach used here is discussed in detail by Kreissl and Maute (2011). A new regularization measure will be introduced and used in concert with a perimeter measure to ensure a well-posed optimization problem. We will study the proposed level set - XFEM approach for both two and three dimensional problems problems and illustrate the influence of regularization methods on the optimized geometry.

The remainder of this paper is organized as follows: in Section 3.1.2, we outline the formulation of the optimization problems considered, the geometry models of density and level set methods.

In Section 3.1.3, the finite element formulations of the governing equations for both material interpolation schemes and the XFEM are presented. In the Section 3.1.4, we compare the temperature predictions for a thick 2D problem using density, Ersatz material and XFEM approaches and present optimization results obtained with proposed level set - XFEM (LS-XFEM) method.

3.1.2 Optimization and Geometry Models

In this section, we first present the formulation of the class of optimization problems considered in this study. This is followed by a brief discussion of the geometry models of density and level set methods.

Optimization Problem

In this study we consider the two and three dimensional problems shown in Figure 3.2. In both configurations a heat flux, q_B, is applied at point B, which is located at the bottom center of the design domain. All walls are considered adiabatic. We seek to minimize the temperature, T_B, at point B with respect to the design variables, $\mathbf{s}$. To regularize the optimization problem, a measure of the perimeter, P, and a gradient measure, G, are introduced into the objective and as constraint. These measures will be discussed in detail in Section 3.1.2. In addition, we constrain the ratio of volumes occupied by the solid and "void" phases. The optimization problem is defined as:

$$\begin{aligned} min_{\mathbf{s}} \quad & p_o\ T_B(\mathbf{s}) + p_p\ P(\mathbf{s}) + p_g\ G(\mathbf{s}) \\ \text{s.t.} \quad & V_1 - V_2 c_v \leq 0, \\ & P - c_p \leq 0, \\ & G - c_g \leq 0, \end{aligned} \tag{3.2}$$

where p_o, p_p and p_g are weights for the temperature, T_B, perimeter, P, and gradient measure, G, in the objective. The solid volume is denoted by V_1, the fluid volume by V_2 , the constrained volume ratio by c_v, the perimeter constraint value by c_p, and the gradient constraint value by c_g. The perimeter and gradient measures are only considered for level set methods; for density methods the corresponding constraints are removed and the associated penalties, p_p and p_g, are set to zero. The temperature field, T, is considered to be dependent on the optimization variable, $\mathbf{s}$, and is governed by the discretized state equation described in Section 3.1.3.

The optimization problem 3.26 is solved by a nonlinear programming (NLP) method. The Globally Convergent Method of Moving Asymptotes (GCMMA) proposed by Svanberg (1995) is applied to the optimization problems here. The design sensitivities are computed using the adjoint method.

Geometry Modeling

In this work we consider density and explicit level set methods. In both methods, the geometry of a body is defined as functions of the optimization variables s_i.

The density method studied below discretizes the material distribution by finite elements. We define an independent optimization variable, s_j at each node. In the thermal finite element analysis the material properties are assumed to be element-wise constant. The element density, ρ_i, of the

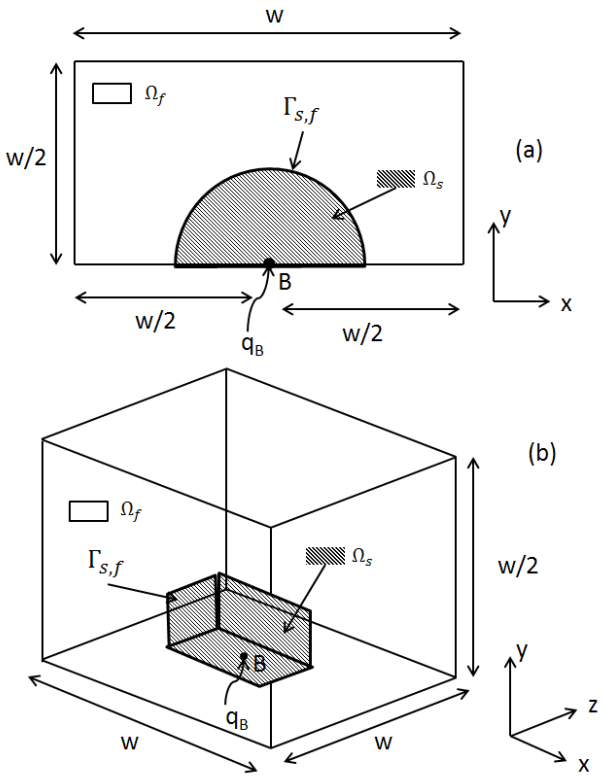

Figure 3.2: Two dimensional (a) and Three-Dimensional (b) Optimization Problem Domains

i^{th} element is computed as follows:

$$\rho_i = \frac{\sum\limits_{j \in I} max\left(0, \left[r - |\mathbf{x}_i - \mathbf{x}_j|\right] s_j\right)}{\sum\limits_{j \in I} max\left(0, \left[r - |\mathbf{x}_i - \mathbf{x}_j|\right]\right)}, \tag{3.3}$$

where the set I contains all nodes within radius r of element i, whose coordinate at center is $\mathbf{x}_i$.

The level set function,ϕ, defines the geometry of the body as follows:

$$\begin{aligned} \phi(\mathbf{x}) &< 0, \quad \forall\ \mathbf{x} \in \Omega_S, \\ \phi(\mathbf{x}) &> 0, \quad \forall\ \mathbf{x} \in \Omega_F, \\ \phi(\mathbf{x}) &= 0, \quad \forall\ \mathbf{x} \in \Gamma_{FS}, \end{aligned} \tag{3.4}$$

where $\mathbf{x}$ denotes the spatial coordinates. The level set function is greater than zero in the fluid phase, Ω_F, less than zero in the solid phase, Ω_S, and equal to zero at the fluid-solid interface, Γ_{FS}.

The level set function is discretized by finite elements and we define an independent optimization variable, s_i, at each node. The nodal values, ϕ_i, of the level set function are computed as follows:

$$\phi_i = \frac{\sum\limits_{j=1}^{N_n} max\left(0, (r - |\mathbf{x}_i - \mathbf{x}_j|) s_j\right)}{\sum\limits_{j=1}^{N} max\left(0, (r - |\mathbf{x}_i - \mathbf{x}_j|)\right)}, \tag{3.5}$$

where the N_n is the total number of nodes and r is the filter radius. The level set field, $\phi(\mathbf{x})$, is interpolated by standard finite element shape functions given the filtered nodal values, ϕ_i.

As discussed by van Dijk et al (2013) and Sigmund and Maute (2013), the level set filter (3.28) does neither guarantee the convergence of the optimized geometry with mesh refinement nor provide local size control. Therefore, perimeter and level set gradient measures will be used in this work to regularize the optimization problem. The perimeter can be conveniently computed by integrating the area along the XFEM interface.

As explained by Burger and Osher (2005) and van Dijk et al (2012), a particularly flat or steep level set field at the interface can lead to poorly scaled sensitivities. To control the level set gradient at the interface a new gradient measure is introduced here as follows:

$$G = \int e^{-\phi^2 e_p^2} \left(|\nabla\phi| - \phi_p\right)^2 d\Omega \tag{3.6}$$

where p is a penalization or steepness measure (typically 10) and ϕ_p is a prescribed level set gradient (typically unity). This measure is introduced in an effort to maintain a sign-distance like level set field near the interface. The measure is composed of two terms, the first exponential approaches zero away from the zero level set and unity nearby. The second term is a measure of closeness to the desired level set gradient. This measure therefore penalizes level set fields that have gradient magnitudes differing from the desired value near the interface.

3.1.3 Thermal Analysis Model

In this section, we introduce the governing equations, summarize two material interpolation approaches to account for convective fluxes at the fluid-solid interface, and outline the XFEM used in this study.

Governing Equations

This work considers a simplified thermal model where the temperature field is modeled by a linear diffusion model. Assuming steady-state conditions, the residual, R_T, of the weak form of the governing equation is:

$$R_T = \int \frac{\partial \delta T_S}{\partial x_i}\ \kappa_{ij,S}\ \frac{\partial T_S}{\partial x_j}\ d\Omega_S + \int \frac{\partial \delta T_F}{\partial x_i}\ \kappa_{ij,F}\ \frac{\partial T_F}{\partial x_j}\ d\Omega_F - \int \delta T_S q\ d\Gamma_q + R_\Omega - R_{FS} = 0 \tag{3.7}$$

with

$$T_F = T_\infty \quad \text{on} \ \in \Gamma_\infty \tag{3.8}$$

where T_k is the temperature in phase k, δT_k the associated test function, $\kappa_{ij,k}$ is the diffusivity tensor in phase k, x_j the j-th spatial dimension, q an applied heat flux, and Γ_q the flux boundary. The contribution, R_Ω, of convective fluxes integrated over the volume of the solid and fluid phase and the contribution, R_{FS}, of the fluxes at fluid-solid interface are defined below. The ambient fluid temperature, T_∞, is imposed at the far walls, Γ_∞. This work will consider isotropic material properties such that

$$\kappa_{ij} = \kappa\delta_{ij}, \tag{3.9}$$

where κ is the diffusion coefficient.

Material Interpolation Approaches

In Section 3.1.4 we will compare for thick 2-D problems the proposed LS-XFEM approach against two approaches that rely on material interpolation schemes. The approach of Moon et al (2004) uses a SIMP method to define the geometry. Yamada et al (2011) use a level set method in combination with an Ersatz material approach. Common to both methods is that the convective flux is approximated via a volume integration and, thus, no contributions. In contrast, the NLC flux is integrated along the fluid-structure interface in the proposed LS-XFEM approach.

SIMP Interpolation Moon et al (2004) present a SIMP interpolation for the thick 2-D configuration. The diffusivity and convection coefficient are interpolated as follows:

$$\kappa = \kappa_0 \rho^p, \tag{3.10}$$

$$h = \left(1 - \rho^{1/p}\right) h_0, \tag{3.11}$$

where κ_0 the diffusivity of the solid material, p the penalization factor, and h_0 the material convection coefficient.

The convective flux is integrated over the design domain. The contribution, R_Ω, in governing equation (3.25) is:

$$R_\Omega = \int_{\Omega_S \Omega_F} \delta T \; h \left(T - T_\infty\right) \; d\Omega \tag{3.12}$$

No convective fluxes along the fluid solid interface are considered. Since the standard finite element interpolation necessarily describes a continuous temperature field along the fluid solid interface, the contribution, R_{FS}, vanishes.

Note that the diffusivity is maximum in the solid phase and vanishes in the fluid phase while the convection is maximum in the fluid phase and zero in the solid phase. Moon et al (2004) argue that embedding these two interpolation schemes into the governing equations (3.25) creates a model where the temperature field in the solid only is influenced by the convective flux in elements with intermediate densities along the interface. The convective flux applied in fluid phase has no influence on the solid temperature due to the vanishing diffusivity in the fluid. The interplay of diffusivity and convection in the fluid phase results in fluid temperature that is approximately equal to the ambient temperature. Therefore, the convection term (3.11) can be interpreted as a penalty method to weakly enforce the ambient temperature in the fluid domain.

Ersatz Material Approach Yamada et al (2011) presents a level-set topology optimization approach where the material parameters are interpolated based on a sign-distance level-set function. The parameters of the Ersatz material approach are interpolated from the level set field, ϕ, by a smoothed Heaviside function, $\tilde{H}$ as follows:

$$\tilde{H}(\phi) = \frac{tanh\left(\beta \phi_t\right) + tanh\left(\beta \left[\phi - \phi_t\right]\right)}{tanh\left(\beta \phi_t\right) + tanh\left(\beta \left[1 - \phi_t\right]\right)}, \tag{3.13}$$

where the parameter β controls the sharpness of the approximation and ϕ_t is the threshold. This function interpolates the density, diffusivity, and convection coefficient as follows:

$$\rho = \frac{\tilde{H}(\phi)}{\tilde{H}(\phi + \phi_t)}, \tag{3.14}$$

$$\kappa = \kappa_{min} + (\kappa_0 - \kappa_{min}) \frac{\tilde{H}(\phi)}{\tilde{H}(\phi + \phi_t)}, \tag{3.15}$$

$$h = h_0 \left| \frac{\partial \phi}{\partial x_i} \frac{\partial \tilde{H}(\phi)}{\partial \phi} \left(\frac{\partial \tilde{H}(\phi_t)}{\partial \phi} \right)^{-1} \right|, \tag{3.16}$$

where κ_{min} is the minimum diffusivity in the fluid phase. In Equations 3.15 and 3.16, the value of the Heaviside function and its derivative are normalized by the value of the Heaviside function at the threshold s_t ensuring a maximum value of unity for each.

As in the interpolation approach of Moon et al (2004), the contributions of the convective fluxes to the residual equation (3.25) are integrated over the entire domain using (3.12) with the convection coefficient being defined by (3.16). Again, the contribution, R_{FS}, of the convective fluxes along the fluid solid interface vanishes.

XFEM

This work uses the XFEM formulation described in detail by Lang et al (2013). In this subsection, we summarize the basic concepts and components. The XFEM augments the space of test and trail functions by additional enrichment functions to capture weak or strong discontinuities within elements intersected by an interface, which is defined by the zero level set iso-contour. In this work we exclusively use Heaviside enrichment functions as they provide great flexibility in discretizing a broad range of partial different equations and in accommodating a variety of interpolation functions (Makhija and Maute, 2013).

Considering a two-phase problem, the temperature field, T, is approximated follows:

$$\hat{T}(\mathbf{x}) = \sum_{m=1}^{M} \left(H(-\phi(\mathbf{x})) \sum_{i}^{N_N} N_i(\mathbf{x}) T_{i,m}^{(1)} + H(\phi(\mathbf{x})) \sum_{i}^{N_N} N_i(\mathbf{x}) T_{i,m}^{(2)} \right), \tag{3.17}$$

where $N_i(\mathbf{x})$ are the nodal basis functions, M the number of enrichment levels, $T_{i,m}^{(p)}$ the degree of freedom at node i for phase p. Here we use an exact Heaviside function, H, which is defined as follows:

$$H(\phi) = \begin{cases} 1 & \phi > 0 \\ 0 & \phi \leq 0 \end{cases} . \tag{3.18}$$

Multiple enrichment levels are necessary for cases where a particular node may interpolate a given phase in more than one patch (separate, disconnected section of material). This ensures that separate patches do not become inadvertently coupled when they are physically disconnected. A detailed explanation of this phenomena is provided by Makhija and Maute (2013). This work considers three different XFEM models to account for convective heat fluxes; see Figure 3.3. The model in Figure 3.3a assumes that the fluid phase is "void". The fluid phase is not considered in the XFEM model and the NLC flux (3.1) is applied along the fluid-solid interface, assuming a constant ambient temperature in the fluid. The contribution to the governing equation (3.25) is:

$$R_{FS} = \int_{\Gamma_{FS}} \delta T_S \; h \left(T_S - T_\infty \right) \; d\Gamma. \tag{3.19}$$

No additional volume contribution, R_Ω, exists.

Alternatively, the model in Figure 3.3b relaxes this assumption and allows for a spatially varying fluid temperature. To this end, we model the fluid phase via a fictitious diffusive material and

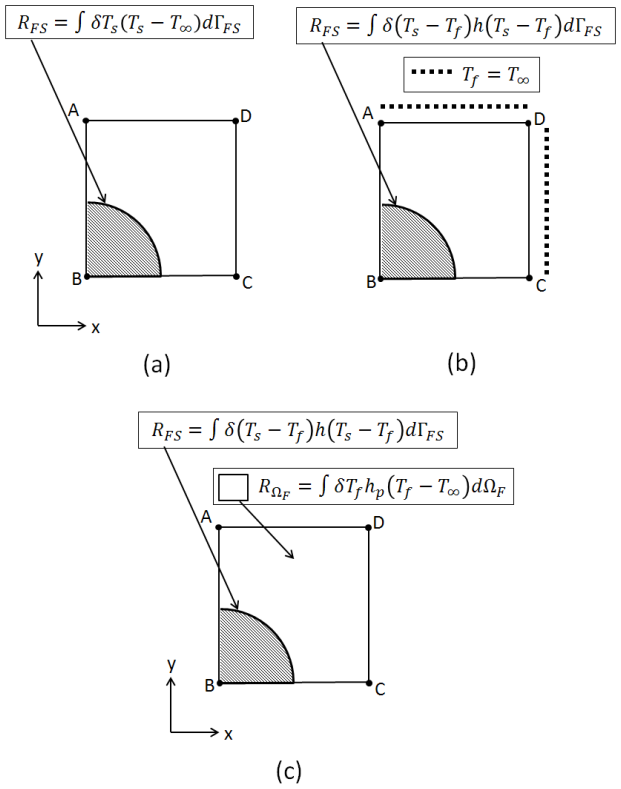

Figure 3.3: True void (a), penalized void (b) and diffusive void (c) XFEM modeling approaches

enforce the ambient temperature in the fluid by applying applying Dirichlet boundary conditions at the far walls, i.e. the design domain boundaries. Note that the larger the diffusivity in the fluid, the smaller is the difference between fluid temperature at the fluid solid interface and the ambient temperature. The flux at the fluid-solid interface leads the following contribution, R_{FS}, to the governing equation (3.25):

$$R_{FS} = \int_{\Gamma_{FS}} \delta T_S \; h \left(T_S - T_F \right) \; d\Gamma - \int_{\Gamma_{FS}} \delta T_F \; h \left(T_S - T_F \right) \; d\Gamma. \tag{3.20}$$

The third XFEM model, as in Figure 3.3c also allows for spatially varying fluid temperature. Here an additional term is added to the residual as:

$$R_{\Omega_F} = \int_{\Omega_F} \delta T_F h_p \left(T_F - T_\infty \right) d\Omega_F \tag{3.21}$$

where h_p is a penalization factor. This convection-like term penalizes the fluid region to drive the temperature towards the far-field fluid temperature T_∞. This model provides two parameters, h_p and κ_F, that will influence the accuracy of the $T_F \approx T_\infty$ assumption on the fluid-solid interface. Increasing values of both should yield the most accurate approximation.

Note the Heaviside enrichment allows for jumps in the temperature field across the fluid-solid interface. As we will show below, relaxing the assumption on the fluid temperature along the fluid solid interface mitigate the emergence of geometric artifacts for the proposed LS-XFEM approach.

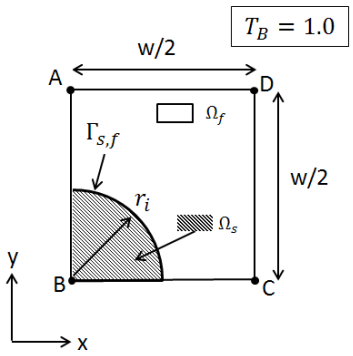

Figure 3.4: Test problem for comparing temperature predictions of material interpolation methods and the XFEM

3.1.4 Numeric Results

The first example (3.1.4) in this section will provide a comparison of temperature fields to show the error resulting from material interpolation approaches and the XFEM. The difficulties of regularizing a poorly-posed problem will be presented with the optimization results of a thick two dimensional problem in Section 3.1.4. Finally the levelset-XFEM will be applied to a three dimensional convection problem (3.1.4) to gauge its performance for the most general problem setup.

Analytical Comparison

Numerical methods for including the NLC flux in a thick two dimensional problem vary substantially in literature. To compare these approaches to the levelset-XFEM the slightly modified convection problem shown in Figure 3.4 is considered. The design geometry is such that the solid material in the domain forms a quarter circle of radius $r = 10.1$ around point B. The total domain width w is 40. The convection coefficient h is 1×10^{-3}, the diffusivity $\kappa = 1.0$ and the ambient fluid temperature $T_\infty = 0.0$. In contrast to the optimization problems of Figure 3.2 the temperature at point B is prescribed as $T_B = 1$. This modification is performed so that temperature fields can be compared more easily as the temperature at B will be the same for all approaches, providing some bound on the field. Applying a flux at B yields temperature fields that appear shifted relative to each other depending on the approach.

As outlined in Table 3.1 a traditional body fitted finite element analysis is compared to five approaches used for topology optimization. The traditional body fitted approach (BF) relies on the creation of surface elements along the solid-fluid interface to incorporate the NLC flux. Method (XL) presents the levelset-XFEM with a true void while (XLD-1) and (XLD-2) are a diffusive void and (XLP-1)-(XLP-4) a penalized void. The design variables for the levelset-XFEM methods are initialized as a sign-distance function and are smoothed with a radius of 1.2.

Methods (M-1) and (M-2) is the Moon-like density method. Design variables corresponding to nodes within the radius $r_i = 10.1$ are set to the minimum value 1.0×10^{-9} while those outside are set to 1.0. The penalty factor p is set to 3.0.

Methods (Y-1) and (Y-2) correspond to the Yamada-like Heaviside interpolation with varying sharpness β of the Heaviside function. The design variables are initialized with a sign-distance function corresponding to the initial radius $r_i = 10.1$ and are smoothed with radius $r = 0.8$. The

Table 3.1: Numeric Approaches for Analytical Comparison

	Approach
BF	Traditional Body Fitted Mesh Finite Element Analysis
XL	Levelset-XFEM with True Void
XLD-1	Levelset-XFEM with Diffusive Void, $\kappa_f = 5$
XLD-2	Levelset-XFEM with Diffusive Void, $\kappa_f = 0.1$
XLP-1	Levelset-XFEM with Penalized Void, $\kappa_f = 5$, $h_p = 1$
XLP-2	Levelset-XFEM with Penalized Void, $\kappa_f = 5$, $h_p = 0.001$
XLP-3	Levelset-XFEM with Penalized Void, $\kappa_f = 0.1$, $h_p = 1$
XLP-4	Levelset-XFEM with Penalized Void, $\kappa_f = 0.1$, $h_p = 0.001$
M-1	Moon-like Density Method, $r = 1.2$
M-2	Moon-like Density Method, $r = 6.4$
Y-1	Yamada-like Interpolation Method, $\beta = 1.0$
Y-1	Yamada-like Interpolation Method, $\beta = 10.0$

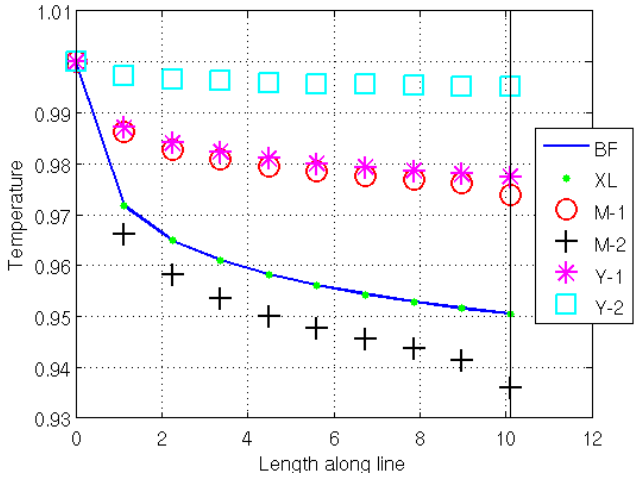

Figure 3.5: Body fitted, XFEM and Interpolation Method Temperature Field Comparison

minimum value of diffusivity $\kappa_{min} = 1 \times 10^{-8}$.

The domain is meshed with 40 quadrilateral elements in each axis for all fixed grid approaches. For the body-fitted finite element method (BF), 20 elements are specified along each axis of the solid domain. For all methods except for (XPD) all walls are considered adiabatic. For the diffusive void XFEM (XLD) walls AD and DC are fixed to $T_\infty = 0$ while BA and BC are adiabatic.

Plotting the temperature along the $x = y$ line in the domain yields Figure 3.5. There is substantial difference between the reference body fitted solution (BF) and the material interpolation methods. The Moon interpolation approach yields a solution that is about half-way between the reference and the prescribed value at B. The Yamada interpolation's agreement varies based on the choice of Heaviside sharpness β, however the correct choice of β is not clear. The appropriate value of β is clouded because resulting flux is a function of both the material interpolation and the element's integration.

Figure 3.6 shows a comparison of the various XFEM approaches. Compared to the material interpolation approaches the levelset-XFEM approaches all match the body-fitted result well. For this simple problem the diffusive void model appears insensitive to diffusivity. The result of both

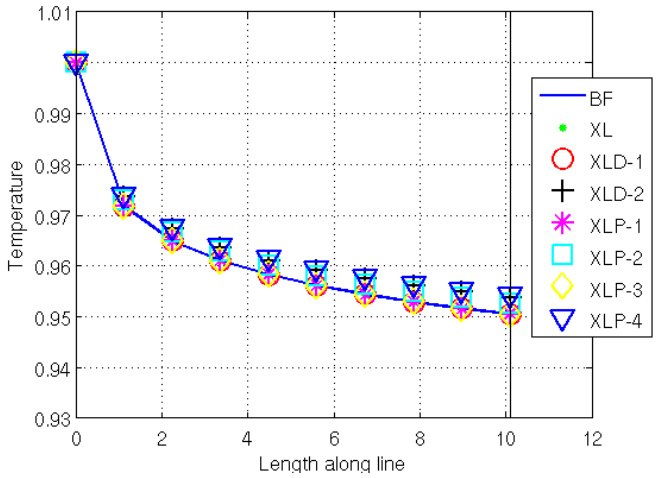

Figure 3.6: Body fitted and XFEM Temperature Field Comparison

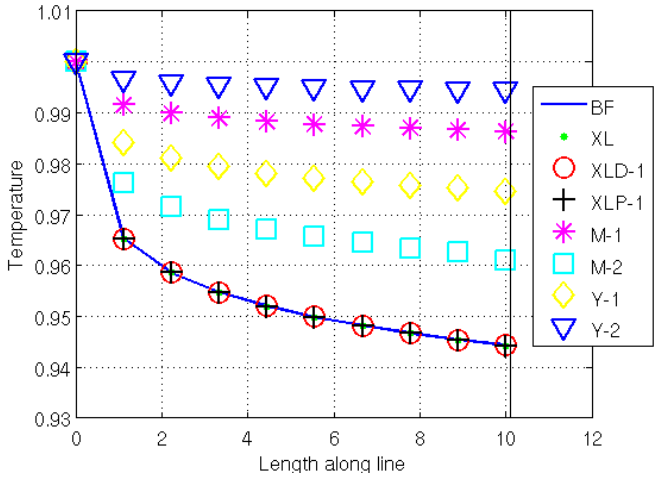

Figure 3.7: Temperature Field Comparison with Refined Mesh

diffusivities are visually identical, however differences in optimization results have been noted. Choice of parameters for the penalized void approach show more variation from the reference solution, though they still are relatively close.

From Figure 3.5 it is clear that the levelset-XFEM approaches well match the reference solution and that the other interpolation methods are of questionable accuracy. Refining the mesh such that elements are of width 0.25 results in the comparison in Figure 3.7. Figure 3.7 shows that with mesh refinement the material interpolation approaches fall even farther away from the reference solution. While this comparison was completed for a thick two dimensional problem, the NLC flux incorporation represents effectively the same problem in the general three dimensional problem. The levelset-XFEM approach therefore appears to be a good choice for the spectrum of two and three dimensional NLC convection problems.

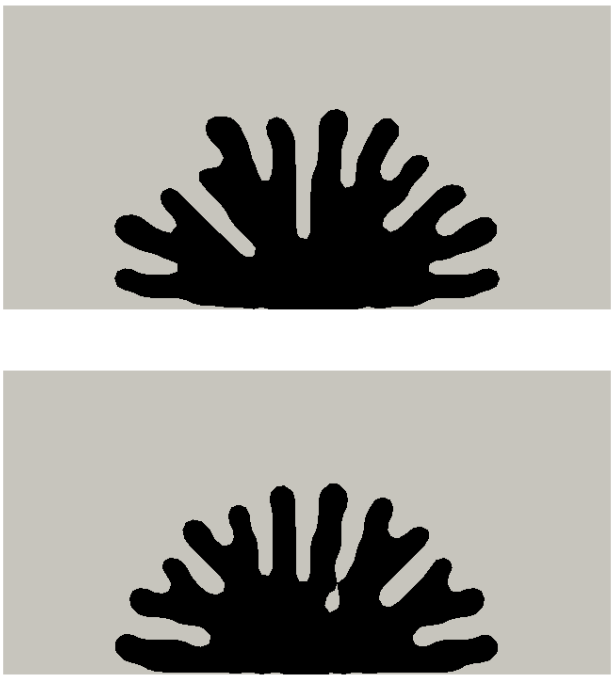

Figure 3.8: Thick two dimensional optimization results using diffusive void (top) and penalized void (bottom) models

Two Dimensional Thick Optimization Problem

The thick two dimensional problem could appear to be a simple extension of the thin problem, however it yields a substantially less well-behaved problem. The symmetry of the $w = 40$ domain is exploited to solve for only half the domain. The domain is meshed with square bilinear elements of height and width 0.5. The ambient Temperature T_∞, flux q_B, convection coefficient coefficient h, solid diffusivity κ, fluid diffusivity and fluid penalization h_p are $[0.0, 1.0, 1.0 \times 10^{-3}, 1.0, 5.0, 1.0]$ respectively. The general problem setup is chosen to match that used in Bruns (2007). The objective scaling p_o, perimeter penalty p_p, gradient measure penalty p_g, perimeter constraint c_p, gradient measure constraint c_g and volume ratio constraint c_v are $[10.0, 1.0 \times 10^{-3}, 1.0 \times 10^{-5}, 50.0, 10.0, 0.3]$ respectively. The smoothing radius r is equal to 1.2 and the initial design is a semi-circle of radius r_i equal to 12.3. The design variables are initialized using a sign-distance function with values limited between -0.33 and 0.33. The design variables beyond a radius of 18 from point B are constrained to remain at their initial (fluid phase) value.

With the appropriate choice of parameters the final designs in Figure 3.8 can be obtained. It is clear that there are a substantial number of parameters to choose and importantly both the perimeter and gradient measure constraints c_p and c_g are active at the final design. Relaxation of the constraints on these measures yields a design problem that does not converge to a final design.

The influence of the constraints on the perimeter P and gradient measure G on the diffusive void model can be seen in Figure 3.9 at design iteration 105. The constraints are relaxed such that $[p_p, c_p, c_g] = [2.0 \times 10^{-3}, 8 \times 10^5, 3.5 \times 10^3]$. The combination of appropriate perimeter and gradient measure constraints discourages the development of thin features in the design that can lead to oscillations. Figure 3.10 shows the same development of thin features when using the penalized

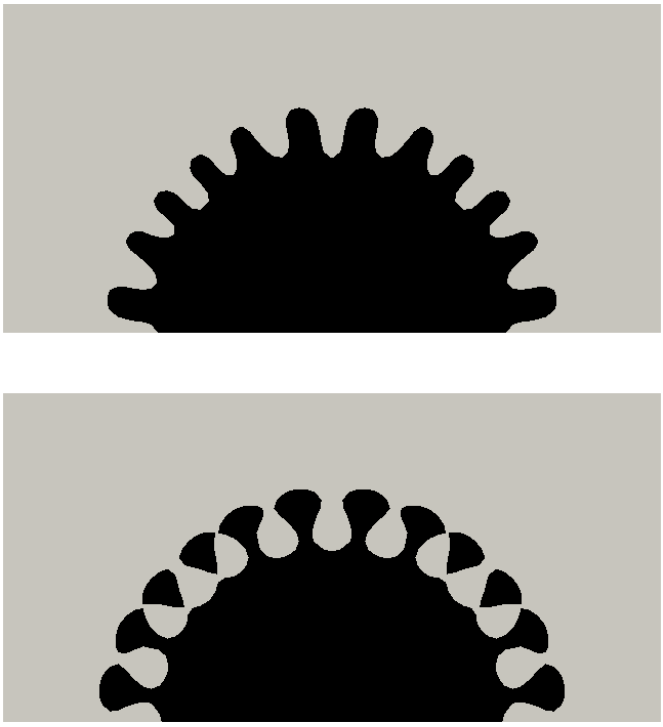

Figure 3.9: Thick two dimensional optimization results using diffusive void model with tight (top) and relaxed (bottom) values of perimeter and gradient measure constraint

void model and relaxing the constraints.

The influence of the thin features on the progression of designs is shown in Figure 3.11. Beneficial thin connections are often overshot by the optimizer leading to disconnected regions. The discontinuous nature of the objective during disconnection and reconnection causes the optimizer oscillate around these designs. The use of more subiterations in the GCMMA algorithm can help limit the oscillation but will not necessarily eliminate the problem. More subiterations in the GCMMA also appears to cause the algorithm to stop at earlier local minima.

In Figure 3.11 there are two sets of thin connections oscillating, those near the base of the structure where the solid region is becoming thin and those near the tips where the fluid-void region is thinning. The thinning of both is a direct result of insensitivity of the heat transfer through a region on its width. The typical nondimensionalization of the conduction-convection problem results in the Biot number:

$$B = \frac{hL_c}{\kappa}, \tag{3.22}$$

where L_c is the characteristic length scale:

$$L_c = \frac{vol}{area}, \tag{3.23}$$

that for a thick semi-circular initial design of radius $\frac{w}{4}$ can be computed as $\frac{w}{8}$. The Biot number can be interpreted as a measure of the relative steepness of the temperature gradient inside the diffusive region. For small Biot numbers the gradients are shallow, leading to insensitivity of the heat transport to the width of certain regions.

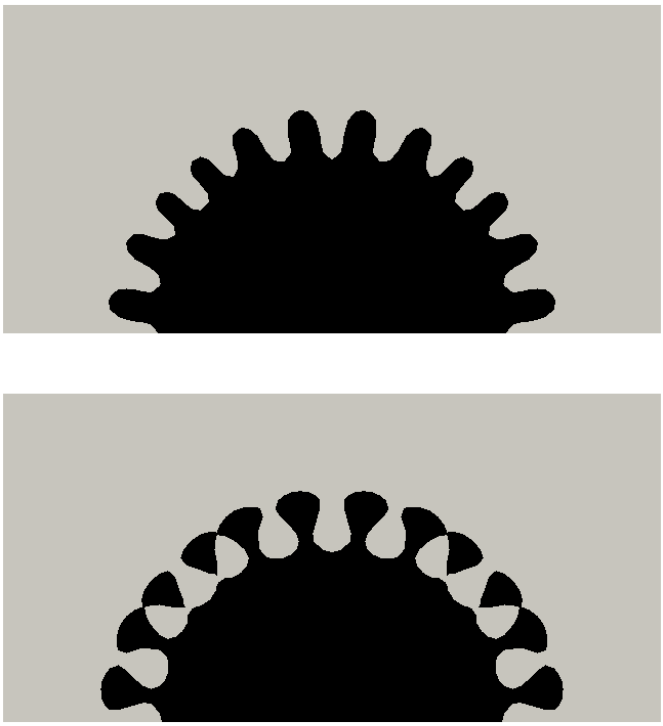

Figure 3.10: Thick two dimensional optimization results using diffusive void model with tight (top) and relaxed (bottom) values of perimeter and gradient measure constraint

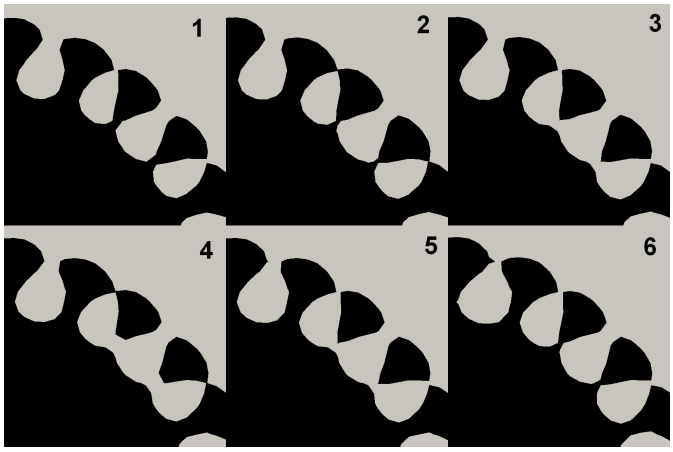

Figure 3.11: Oscillations in design iterations due to thin features

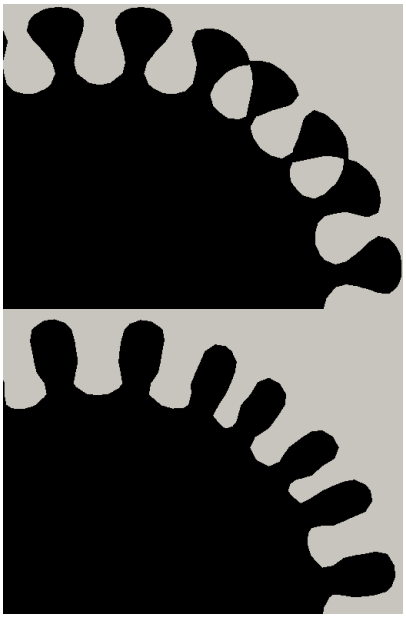

Figure 3.12: Comparison of intermediate design for two Biot numbers, 0.005 top, 0.5 bottom

The thinning of solid regions near the base of structures is a result of the low Biot number in the solid region. The resulting thicker solid structures resulting from a larger Biot number are seen in Figure 3.12. Our previous problem (3.12 top) yields a Biot number of 5×10^{-3}, similar to a $2cm$ cube immersed in air. The large value of Biot number (3.12 bottom), 0.5 is consistent with a $20cm$ cube of steel immersed in water. It is clear that for systems with larger Biot numbers the design problem is more well behaved. Unfortunately large values of Biot number will still yield problematic thin connections in the fluid region.

The thinning fluid-void is a result of the large diffusivity (and therefore small Biot number) in the fictitious fluid-void domain used to provide good enforcement of the NLC condition at the interface. While the Biot number for solid region ($\kappa = \kappa_s$) is dependent on the problem setup, the Biot number of the fluid-void region ($\kappa = \kappa_F$) is free to the designer, a non-physical parameter that influences that quality of the NLC condition at the interface. Again using the Figure 3.9 bottom as reference, the ratio of κ_F/κ_S is lowered, showing in Figure 3.13 the relative thickening of the fluid regions.

Other modifications of the problem parameters can yields models that represent completely different physical problems. For large values of convection coefficient the NLC flux at the solid-fluid interface behaves like a penalty measure enforcing continuity in the temperature field. Choosing values of $[\kappa_f, h_p, h] = [0.1, 1 \times 10^{-3}, 1]$ the physical problem becomes that of a purely diffusive system. The values of κ and κ_f are roughly equivalent to immersing a metal in water. Lacking advection in the fluid phase the model is restricted to problems with little fluid motion. With relaxed constraints $[p_p, c_p, c_g] = [2.0 \times 10^{-3}, 8 \times 10^5, 3.5 \times 10^3]$ this model still leads to a well behaved design problem shown in Figure 3.14. In the purely diffusive problem it is beneficial to build solid structures reaching out towards the T_∞ heat sink. Using the diffusive void model in the top image of Figure 3.14 the structures reach towards the outer walls where $T_f = T_\infty$. The structures thicken at their extents where they reach the fixed design region at a radius of 18. The penalized void model enforces $T_f = T_\infty$ by penalization through the fluid domain yielding structures that provide more evenly cover the fluid domain.

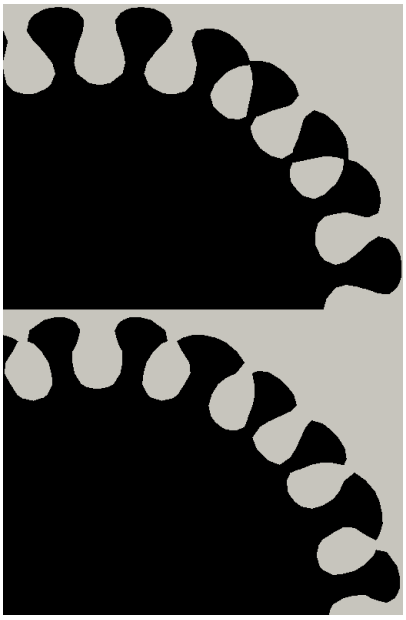

Figure 3.13: Comparison of intermediate design for varying fluid diffusivity, $\kappa_F/\kappa_S = 5.0$ top, $\kappa_F/\kappa_S = 0.05$ bottom

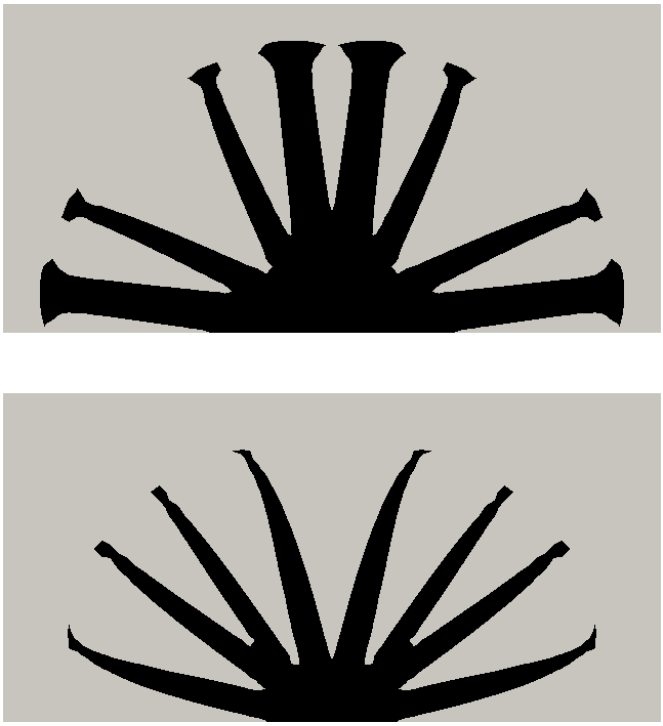

Figure 3.14: Thick two dimensional optimization results using relaxed physical modeling similar to a purely diffusive problem, $[\kappa_f, h_p, h] = [0.1, 1 \times 10^{-3}, 1]$, diffusive void top, penalized void bottom

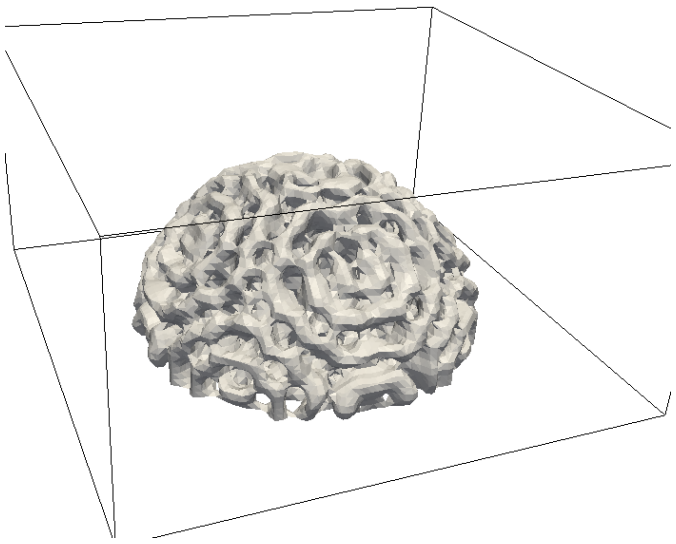

Figure 3.15: Three Dimensional Edge Convection via Convection Neumann Boundary Condition on XFEM Interface via Diffusive Void

Three Dimensional Optimization Problem

The three dimensional optimization problem is solved on a $20 \times 20 \times 20$ domain, exploiting quarter symmetry of full $w = 40$ domain in Figure 3.2 (B). The domain is meshed with cubic eight-node hexahedral elements of height, width and depth equal to 0.5. The material parameters are again $[T_B, q_B, h, \kappa, \kappa_f] = [0.0, 1.0, 1.0 \times 10^{-3}, 1.0, 10.0]$. The optimization parameters are $[p_o, p_p, p_g, c_p, c_g, c_v] = [10.0, 1.0 \times 10^{-3}, 1.0 \times 10^{-5}, 325.0, 200.0, 0.3]$. The smoothing radius is $r = 0.01$, yielding effectively no smoothing. The design variable bounds are $[-0.2, 0.2]$.

The resulting design from the three dimensional NLC convection problem is shown in Figure 3.15. The only active constraint for this final design is that of the perimeter. Compared to the optimization in of the thick two dimensional problem in Section 3.1.4 the three dimensional optimization problem appeared to less sensitive to the regularization parameters.

Figure 3.16 shows a three dimensional NLC convection result using the same relaxed set of parameters of Figure 3.14 (top). In three dimensions the same affinity to developing long fingers is shown. The fingers clustering to parts of the domain where the limited radius is closest to the outer walls.

3.1.5 Conclusions

The levelset-XFEM approach has been shown to be particularly effective at accurately modeling the NLC convection conditions enforced on the embedded design interface. Existing density method approaches for modeling a thick two dimensional problem were shown to have substantial errors in the resulting temperature field for a particular design. Unfortunately the design problem resulting from NLC convection is poorly behaved. This study suggests that resolving the fluid in the convection problem will result in a more suitable problem for topology optimization. Resolution of the fluid will naturally discourage features that would be undesirable but are beneficial in the NLC problem. Due to the form of the levelset-XFEM approach it is possible to separate approximations in the physics modeling from the design problem. This separation has allowed for a better understanding of the behavior of the NLC convection optimization problem.

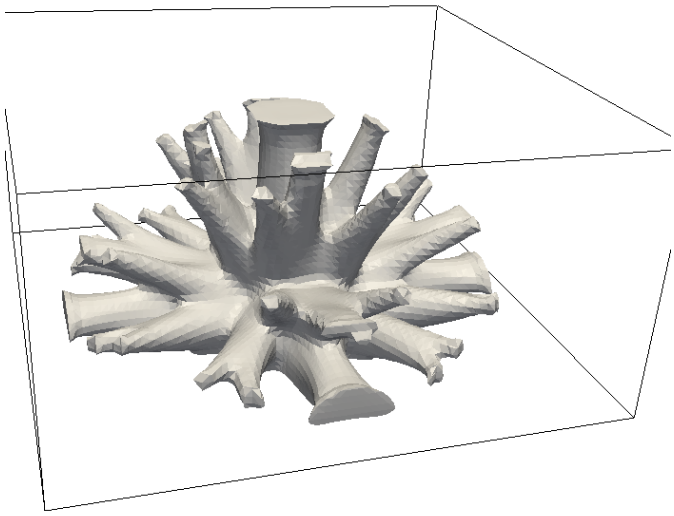

Figure 3.16: Three Dimensional Edge Convection via Convection Neumann Boundary Condition on XFEM Interface via Relaxed Diffusive Void

3.2 Topology Optimization of Natural Convection Problems

3.2.1 Introduction

Heat transport is an important design consideration in many devices. Heat is often an unwanted byproduct of operation and if unmanaged can yield high temperatures that degrade performance or shorten service life. The process of convection, transfer of heat via fluid motion is a phenomena commonly exploited for device cooling and as has been incorporated into a number of previous optimization works such as those by Bruns (2007) and Morrison (1992).

As device design advances, topology optimization can play an important role in helping develop better performing designs. Topology optimization as pioneered by Bendsøe and Kikuchi (1988) for solid mechanics problems is a particularly general approach to optimization that allows for a general material distribution in a given design domain. More simple design optimizations as in Morrison (1992) and Bahadur and Bar-Cohen (2005) vary particular geometric features such as the number of cooling fins and their length and width. While these approaches benefit from decreased computational cost, their natural constraints on design geometry (due to the embedded geometry definitions) allow topology optimization approaches to excel by exploring additional design space that can result in unanticipated and unintuitive designs.

In a convection problem heat transport must be considered in three distinct domains, the solid, the moving fluid and the boundary between the two. A common approach to simplify this analysis is to ignore the fluid domain, prescribing a temperature dependent flux according to Newton's Law of Cooling (NLC) at the fluid-solid interface. A number of topology optimization works including those of Bruns (2007), Yin and Ananthasuresh (2002) and Alexandersen et al (2013) have considered NLC convection models. Key to Newton's Law of Cooling is the knowledge of the correct value of convection coefficient, which is a function of the surface geometry, fluid motion, and fluid material properties (Cengel et al, 1998). As the surface geometry and resulting fluid motion will likely change with varying optimization designs, this assumption is a potential source

of error in the temperature field. To maintain the most accuracy, this work will model the entire coupled fluid-solid system.

Convection problems can be broken into two categories, forced or natural. Forced convection problems are those where the fluid motion is driven by some external source (i.e. a fan). Natural convection problems are the more challenging, fully-coupled problem where fluid motion is completely driven by the temperature dependent buoyancy forces. Topology optimization of forced convection problems has been the target of a few works, notably Pingen and Meyer (2009). Natural convection has seen less attention with Alexandersen et al (2014) being the only known example. The fully-coupled natural convection problem will be the target of this work.

One discretization approach for topology optimization is the density or SIMP (Solid Isotropic Microstructure with Penalisation) method, originally proposed by Bendsøe (1989) and pioneered by the works of Zhou and Rozvany (1991) and Rozvany et al (1992). Originally developed for solid mechanics this approach has been applied to a number of different physics including structures, heat transfer, and fluids (Bendsøe and Sigmund, 2003)(Sigmund and Maute, 2013). Alexandersen et al (2014) use this approach for the natural convection problem. Their work notes one of the primary difficulties of density approaches, intermediate materials that yield unphysical but beneficial characteristics to the objective.

An alternative approach to discretely defining the material distribution is using levelsets. The levelset of a higher order field is used to define the boundary between two material phases. This approach conveniently eliminates the concept of intermediate material and provides an implicit definition of the interface. The levelset optimization problem can be directly updated by solving a Hamilton-Jacobi-like equation as in Wang and Wang (2004) or as used here, by explicitly defining the levelset field as a function of a set of design variables (de Ruiter and van Keulen, 2001). Explicit definition of the levelset field allows the use of typical mathematical programming techniques as described by van Dijk et al (2013). The immersed boundaries resulting from the levelset approach are handled using the eXtended Finite Element Method (XFEM), which was originally developed for modeling the discontinuous behavior of cracks in solid mechanics by Belytschko and Black (1999), Moes et al (1999) and Daux et al (2000). This approach enriches the standard finite element interpolation functions near the boundary with additional functions and degrees of freedom to allow for modeling of discontinuities in the interpolated field.

In this work the topology optimization of a natural convection cooling device will be explored using an explicit levelset-XFEM approach. The explicit levelset-XFEM approach is introduced to help alleviate unphysical effects of intermediate material in the design domain and produce a crisp boundary definition throughout the optimization process. The influence of steady-state and transient analysis on a seemingly steady-state problem will be explored in two dimensions, along with the behavior of a fully transient problem in two dimensions and a steady-state problem in three dimensions. In Section 3.2.2 the physical optimization model problem and relevant equations will be described. The process of discretization for the explicit levelset and XFEM will be described in Section 3.2.3. Numerical results from the three example problems (steady-state two dimensional, steady state three dimensional and transient two dimensional) will be shown in Section 3.2.4. Finally a discussion of the results will be made in Section 3.2.5.

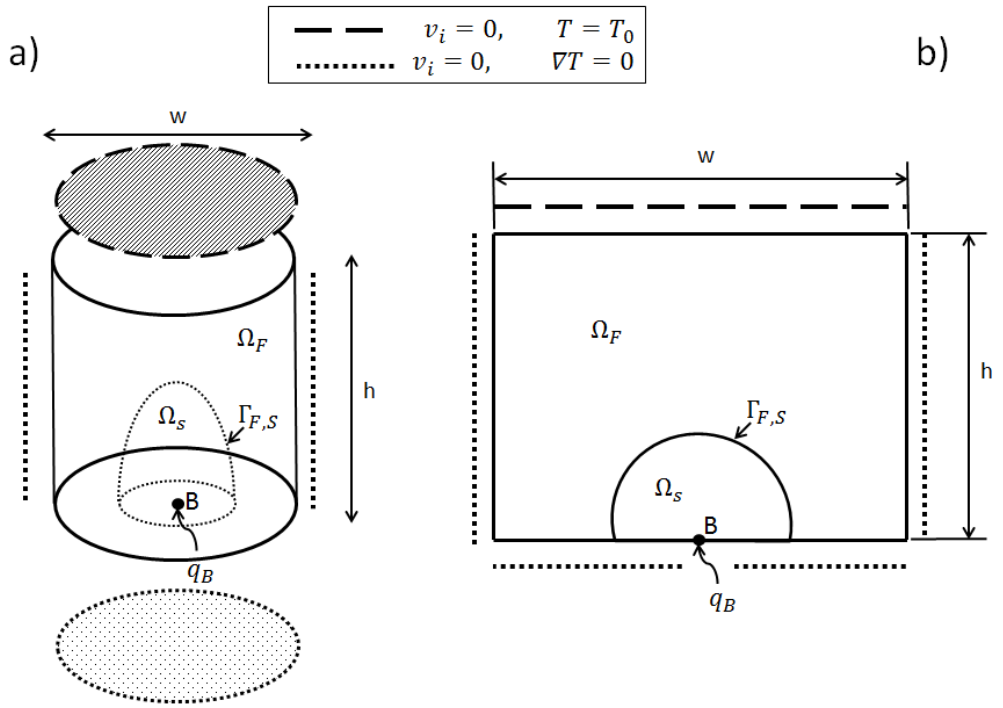

Figure 3.17: Three (a) and two dimensional (b) natural convection problem layouts

3.2.2 The Model Problem

The Analytical Problem

Figure 3.17 shows both a three and two dimensional layout of the natural convection problem. The three dimensional layout consists of a cylinder of diameter w and height h with a heat flux q_B applied at point B. The two dimensional layout is a rectangular box of width w and height h. Surrounding point B is a region of solid material Ω_s that is immersed in fluid Ω_f, the boundary between them being $\Gamma_{s,f}$. In both configurations the temperature on the top surface is fixed to T_0. The side and bottom walls are adiabatic. The fluid velocity at all walls and the fluid-solid interface is zero.

The natural convection system is governed by two sets of equations, one defining the fluid motion 3.24 and one defining the transport of the temperature through the system 3.25. The equations will be solved in space using finite elements and in time using a standard implicit first order backwards formula. We define a general advection-diffusion equation, applicable both to the fluid domain and to the solid domain. In the solid domain the advection velocities will be exactly zero. The weak, residual form of the fluid governing equations are:

$$R = \int w_i \rho \frac{\partial v_i}{\partial x_j} v_j d\Omega_f - \int \frac{1}{2}\left(\frac{\partial w_i}{\partial x_j} + \frac{\partial w_j}{\partial x_i}\right) p\delta_{ij} d\Omega_f + \int \frac{1}{2}\left(\frac{\partial w_i}{\partial x_j} + \frac{\partial w_j}{\partial x_i}\right) 2\mu \frac{1}{2}\left(\frac{\partial w_i}{\partial x_j} + \frac{\partial w_j}{\partial x_i}\right) d\Omega_f + \int w_i \rho g_i \left(1 - \alpha_{TE}\left[T - T_0\right]\right) d\Omega_f + \int q \frac{\partial v_i}{\partial x_i} d\Omega_f - \int w_i n_j \left(-p\delta_{ij} + 2\mu \frac{1}{2}\left[\frac{\partial v_i}{\partial x_j} + \frac{\partial v_j}{\partial x_i}\right]\right) d\Gamma_{f,s} = 0 \quad (3.24)$$

where Ω_f is the fluid domain, $\Gamma_{f,s}$ the fluid domain boundary, w_i are the velocity test functions, ρ the fluid density, v_i the fluid velocity, p the fluid pressure, q the pressure test functions, μ the fluid dynamic viscosity, g_i the gravitational accelerations, α_{TE} the coefficient of thermal expansion, T the temperature, T_0 the reference (zero-expansion) temperature and n_j the interface normal. As the weak form is discretized using bilinear, quadrilateral elements for both velocity and pressure, the SUPG/PSPG-stabilization of Tezduyar (1992). An additional term containing the buoyancy effects, dependent on g_i is noted, which drives the fluid motion according to the temperature differences.

The standard weak form of the advection-diffusion equation is:

$$R = \int m\rho c_p \frac{\partial T}{\partial t} d\Omega \int m v_j \frac{\partial T}{\partial x_j} d\Omega + \int \frac{\partial m}{\partial x_j} k \frac{\partial T}{\partial x_j} d\Omega = 0 \quad (3.25)$$

where m is the temperature test function, k the material diffusivity, q_b a body flux term and q_e a boundary flux term. SUPG stabilization is applied, as earlier, to the convective portion of this residual as well. Ω is considered to be the entire fluid-solid domain. Handling of the eXtended Finite Element Method and immersed boundaries will be discussed in 3.2.3.

The Optimization Problem

The goal of this work is to optimize the topology of a cooling device, such that where a heat flux enters the system, the temperature is kept to a minimum. This is analogous to trying to minimize the working temperature of a computer CPU that produces a given amount of heat while under load. The material properties for the problem are chosen so they correspond to physically meaningful values; the fluid being air, the solid being aluminum and the length scale 3 cm. The magnitude of heat flux is then used to scale the system and explore the complexities that arise from more substantial heat transfer and fluid motion. The temperature used in the objective function is evaluated at the final time step of the solution.

The general topology optimization problem is stated as,

$$\begin{array}{ll} min_{\mathbf{s}} & p_o T_B(\mathbf{s}, \mathbf{u}) + p_p P \\ \text{s.t.} & \mathbf{R}(\mathbf{u}, \mathbf{s}) = 0 \\ & V_s - c_v \leq 0.0 \\ & P - c_{pe} \leq 0.0 \end{array} \quad (3.26)$$

where one is minimizing the temperature at B with respect to the design variables $\mathbf{s}$ and states $\mathbf{u}$, subject to satisfying the residual equations and the inequality constraints on the solid volume V_s and the interface perimeter P. Values of c_{pe} and c_v are the maximum allowed perimeter and

volume ratio respectively. The objective also incorporates tunable penalties for the perimeter, such that p_o and p_p are the scaling coefficients for the temperature and perimeter.

3.2.3 Discretized System Details (Levelset-XFEM)

Levelset Optimization Approach

The material phases are described using the explicit levelset approach as

$$\begin{aligned} \phi(\mathbf{x}) &< 0, \quad \forall\ \mathbf{x} \in \Omega_s, \\ \phi(\mathbf{x}) &> 0, \quad \forall\ \mathbf{x} \in \Omega_f, \\ \phi(\mathbf{x}) &= 0, \quad \forall\ \mathbf{x} \in \Gamma_{s,f}, \end{aligned} \tag{3.27}$$

where $\mathbf{x}$ is the spatial coordinate, Ω_s is the solid phase, Ω_f the fluid phase and $\Gamma_{s,f}$ the boundary between the solid and fluid phases. The discrete optimization variables s_j are defined nodally and filtered so that nodal levelset values ϕ_i can be computed according to:

$$\phi_i = \frac{\sum_{j=1}^{N} max\left(0, (r_s - d_{ij}) s_j\right)}{\sum_{j=1}^{N} max\left(0, (r_s - d_{ij})\right)} \tag{3.28}$$

where r_s chosen filter radius and d_{ij} is the distance from node i to node j. The value of levelset ϕ is computed for any spatial point using the standard finite element shape functions. This explicit levelset approach has been used by a number of authors such as Wang and Wang (2006), Luo et al (2007) and Pingen et al (2010) and allows for the use of traditional mathematical programming schemes.

XFEM Discretized System

The XFEM approach of this work is proceeded and explained in detail by the earlier works of Kreissl and Maute (2012) and Lang et al (2013), who considered incompressible Navier-Stokes and diffusion problems respectively. In this work the two physics are coupled by the addition of advection to the diffusion problem and temperature dependent buoyancy terms to the incompressible Navier-Stokes problem. The general XFEM approach used is to augment the normal finite element interpolation schemes by additional enrichment functions and degrees-of-freedom. Heaviside step enrichment is used as a flexible approach applicable to many problems as described by Makhija and Maute (2013), where the enriched interpolation of u, $\hat{u}$ is

$$\hat{u}(\mathbf{x}) = \sum_{m=1}^{M} \left(H(-\phi(\mathbf{x})) \sum_{i \in I} N_i(\mathbf{x}) u_{i,m}^{(1)} + H(\phi(\mathbf{x})) \sum_{i \in I} N_i(\mathbf{x}) u_{i,m}^{(2)} \right) \tag{3.29}$$

for two material phases, where I is the set of all nodes, $N_i(\mathbf{x})$ the nodal basis functions, M the number of enrichment levels, $u_{i,m}^{(p)}$ the degree of freedom at node i for phase p, and H the Heaviside function,

$$H(z) = \begin{cases} 1 & z > 0 \\ 0 & z \leq 0 \end{cases} . \tag{3.30}$$

Makhija and Maute (2013) describe the need for multiple enrichment levels to alleviate unintentional coupling between disconnected patches of material. The final component of Heaviside XFEM is to enforce necessary continuity across the XEM interfaces. The stabilized Lagrange multiplier technique is a common approach to enforcing interface constraints in the XFEM. The general approach is described by Stenberg (1995), while the approach applied to the diffusion problem is described by Lang et al (2013) and to fluid problems by Gerstenberger and Wall (2008), Gerstenberger and Wall (2010) and Kreissl and Maute (2012).

3.2.4 Example Problems

Three optimization problems are considered to explore the complexities of natural convection systems. The first problem (3.2.4) consists of a two dimensional box with steady state flow due to a small value of q_B. The second problem (3.2.4) models the general three dimensional system with steady state flow due to a small value of q_B. The final example (3.2.4) considers a system that yeilds unsteady flow due to a larger value of q_B and box dimensions.

For this work the Globally Convergent Method of Moving Asymptotes of Svanberg (1995) is used. A transient adjoint sensitivity analysis is performed according to Kreissl and Maute (2012).

Two Dimensional Box Simple Problem

The first and simplest numerical example is described in Table 3.2 and Figure 3.18. The heat flux q_B is chosen such that for the initial design the fluid flow achieves a steady state solution with a resulting Grashoff number of 9.9×10^3. Allowing the optimizer to proceed for 708 iterations yields the right-hand design in Figure 3.18, which decreases the temperature at the applied flux from 2.7119 in the initial design to 2.3639. A visually identical design is reached after only 300 iterations with a similar temperature of 2.3641. The GCMMA relative step size is set to 0.02 and the asymptotes to [0.5,0.7,1.43]. Symmetry on the design is enforced for the example in Figure 3.18 by only defining one set of design variables s_n corresponding to nodes on the left half of the domain and mapping their influence to the corresponding node on the right half of the domain.

One key behavior in the natural system is that a steady state solution does not indicate that the steady state solution found is stable. In Figure 3.19 a comparison is shown between the solution of the natural convection problem with a given initial design for both a steady state assumption and a transient analysis ($\Delta t = 10.0$, $t_{max} = 1.999 \times 10^4$). The flow pattern of the two is clearly different, the steady state analysis finding a symmetric solution while the transient analysis driving towards an unsymmetric pattern. During the transient analysis the symmetric flow pattern is initially exhibited until switching at a particular time value, after which the solution retains the same flow pattern.

Three Dimensional Box Problem

The natural convection problem of Section 3.2.4 is extended to three dimensions by rotating about the center, resulting in a cylindrical design domain. The approach to the problem is identical to the previous two dimensional example with the primary difference being the much more substantial computational time and less stable nonlinear equation to solve. The initial results shown here in Figure 3.20 appear reasonably well formed and while thin, disconnections and reconnections do not appear to be an issue as with the NLC design problem.

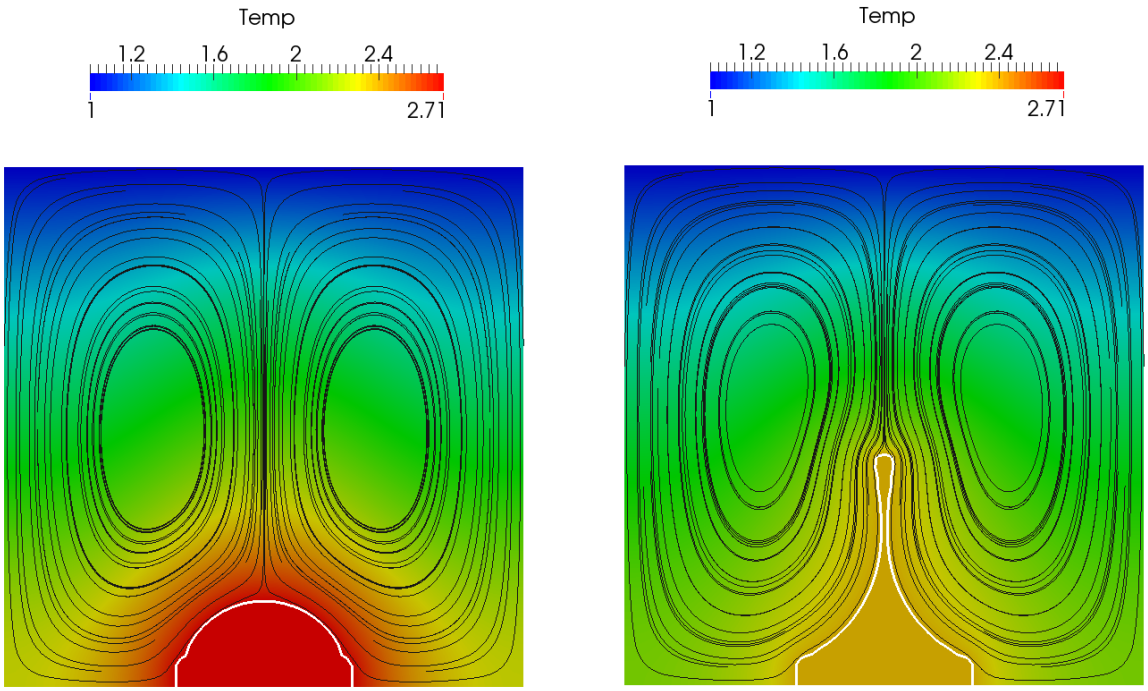

Figure 3.18: Initial (left) and Final (right) Designs for Two Dimensional Steady State Natural Convection Problem

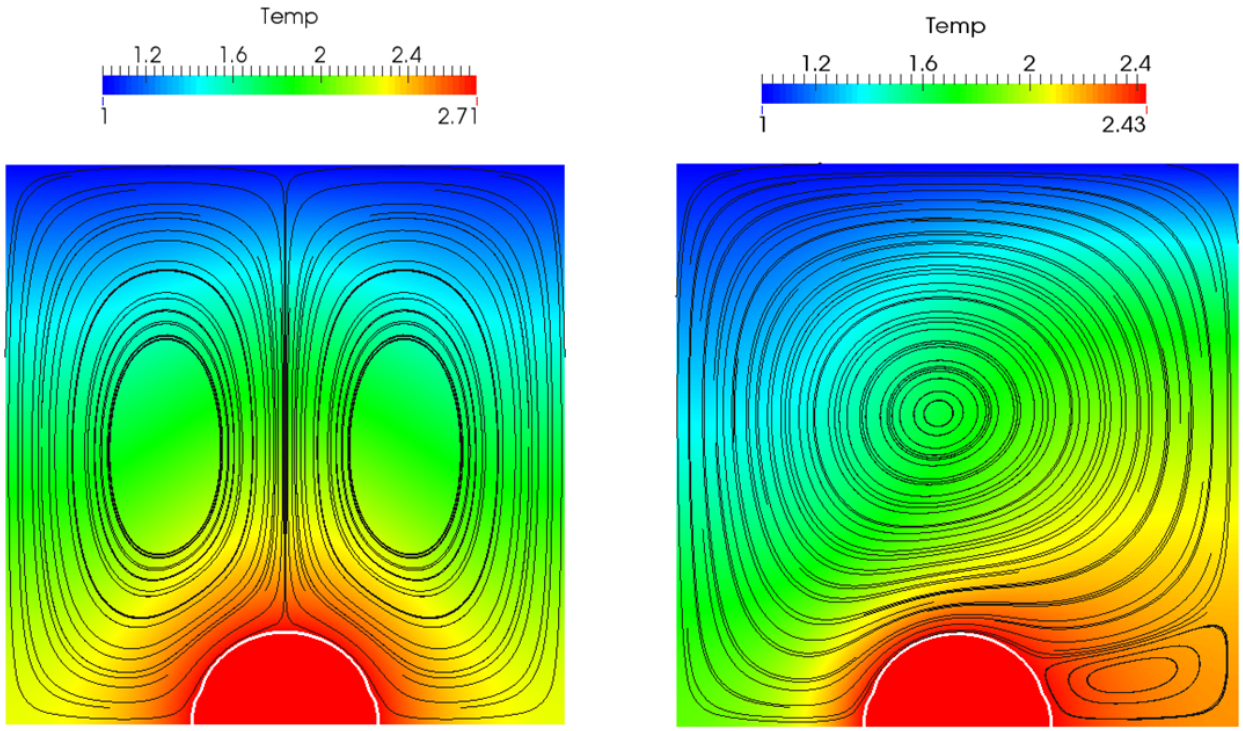

Figure 3.19: Steady state (Left) and transient (Right) analysis results for a particular initial design

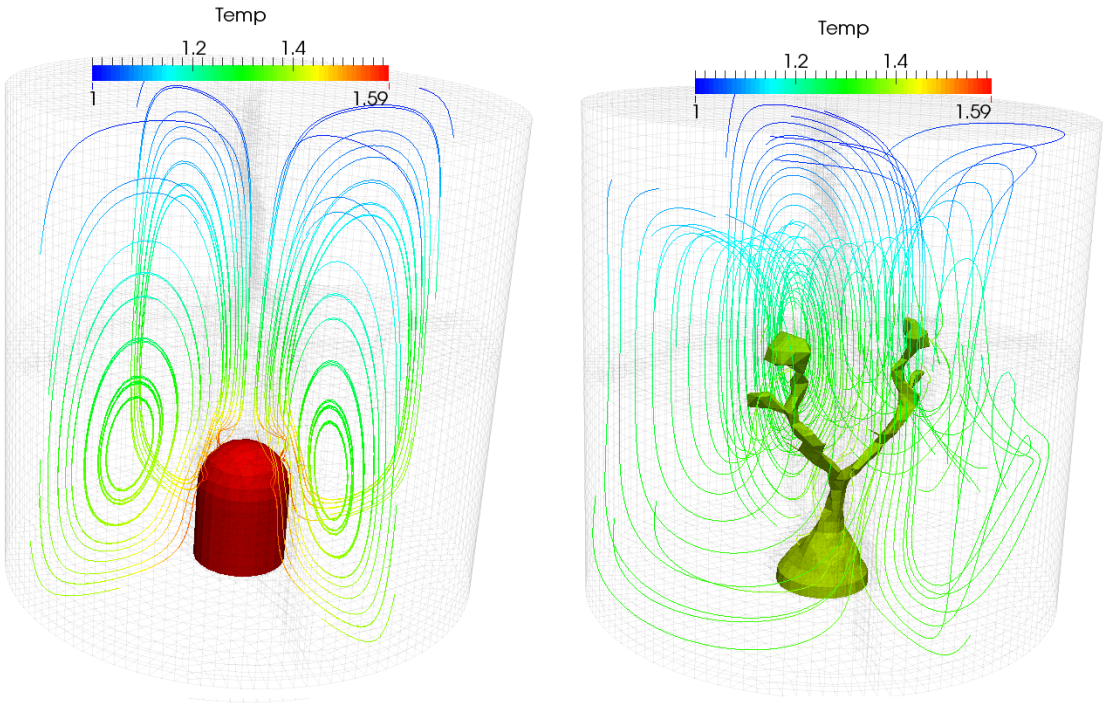

Figure 3.20: Initial (left) and Final (right) Designs for Three Dimensional Steady State Natural Convection Problem

Two Dimensional, Highly Transient Problem

As indicated previously the current framework is capable of analyzing a fully coupled, transient, natural convection problem. A natural extension of the previous two-dimension example is used here, expanding the dimensions of the box and increasing the applied flux, yielding an intial Grashoff number of 3.9×10^6. At the initial design the flow develops into a long, thin column that continually switches orientation as the vortices at the top of the box switch positions. The initial and final designs for this problem are shown in Figure 3.21 at the final time step of the analysis.

The optimizer succeeds in decreasing the target temperature from 254 to 58 over the course of the optimization. The final design for this problem retains substantially more bulk at the top of the fin as compared to the examples in Section 3.2.4. Unfortunately the computational cost of this optimization becomes particularly substantial due to the time resolution necessary. The time step necessary to resolve the transient behavior visible in the flow was 1.0 and to achieve a somewhat steady result in the temperature of interest a total of 2500 was needed. Combined with the mesh refinement necessary to resolve the flow (25k degrees of freedom) meant that even with a time iteration taking about one second, the total time for a forward and sensitivity analysis would be 1.5 hours. This was performed on a six core desktop in parallel and it was found that due to communication overhead moving to a cluster with a larger number of nodes was ineffective in decreasing the computational time.

3.2.5 Discussion

The examples in this work clearly show that the levelset-XFEM can be well applied to natural convection problems and that the inclusion of transient analysis is important. Even for problems

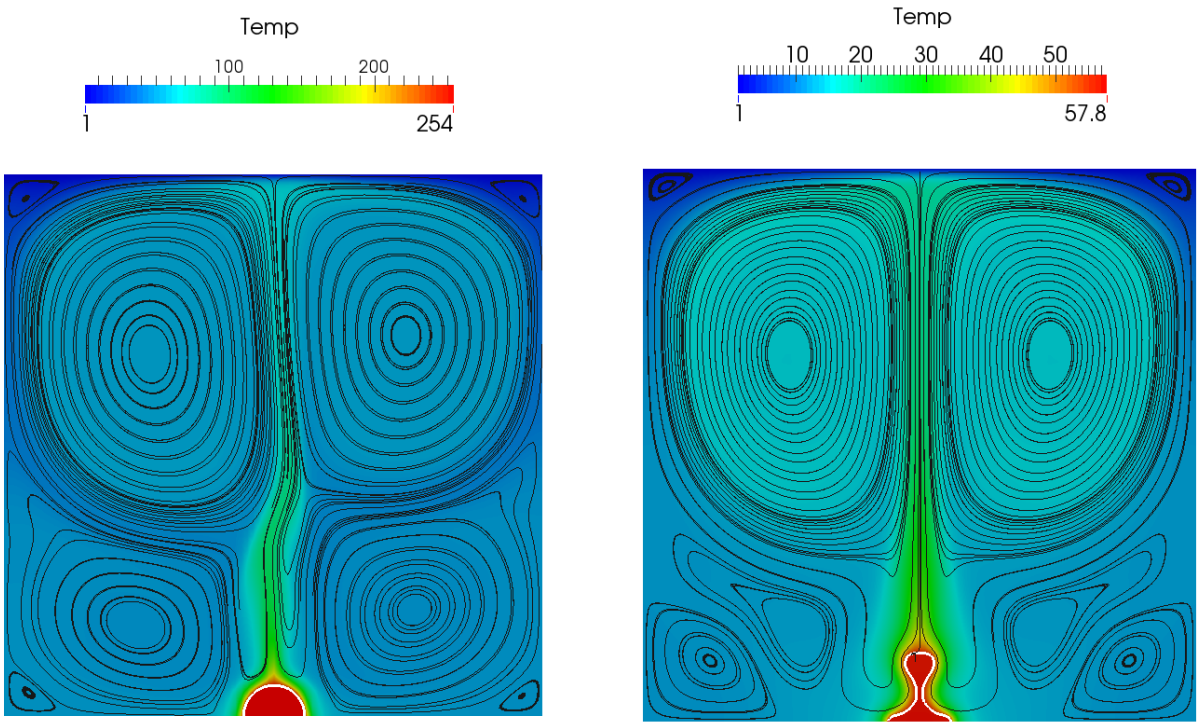

Figure 3.21: Initial (left) and Final (right) Designs for Two Dimensional Transient Natural Convection Problem

where the steady-state analysis yielded the same result as long-term transient analysis it was found that transient analysis was substantially more robust considering the range of designs that were produced during an optimization. A coarse transient analysis could be considered an alternative to the combined, highly damped newton solve and ramped forcing used by Alexandersen et al (2014).

The substantial cost associated with the full transient example problem was partially due to the consistent time step used through the simulation. An intelligent adaptive time stepping scheme could have at least eliminated some fine stepping completed before the flow had developed its unsteady behavior. More than half of the total simulation time exhibited this unsteady behavior so the effect would certainly be limited. Further study of problem setup and initialization and time discretization methods should certainly be considered for further work.

The levelset-XFEM approach eliminated the difficulties described by Alexandersen et al (2014) of penalizing intermediate, porous material with internal natural convection. Poorly intersected elements (small ratios of volume of one material phase to another) did create difficulties however that would yield poor solutions and poorly scaled sensitivities. This issues was generally resolved by applying the preconditioning approach of Lang et al (2013). Poor scaling of equations solved for the enforcement of interface fluid velocities would still sometimes yield designs whose analysis would not converge well. This was generally solved when the optimizer would take the next step and the intersections would change slightly.

The regularization of the levelset field also provided challenges during the optimization as the natural convection system would often lead to thin features in the solid domain. It could be considered that this was generally driven by the high conductivity in the solid domain combined with the magnitude of heat transfer depending on the interface area. A traditional regularization, the

perimeter was chosen as both a penalty and constraint and was generally effective at helping yield sensible designs. A convenient parameter that more directly measures the geometry of interest, feature size, would be a welcome addition to the levelset-XFEM approach.

Table 3.2: Example Problem Parameters

Value	2D Box	3D Box	2D Tall Transient
h	0.03	0.03	0.09
w	0.03	0.03	0.09
d_f	0.00125	0.00125	0.00125
r_f	0.0025	0.0025	0.0025
r_i	0.005	0.005	0.005
r_s	-tbd-	-tbd-	-tbd-
q_B	0.05	3.33×10^{-4}	50.
p_p	1×10^{-4}	1×10^{-4}	1×10^{-4}
p_o	1.0	1.0	1.0
c_v	3.927×10^{-5}	5.24×10^{-7}	3.927×10^{-5}
c_{pe}	0.0314	3.1415×10^{-4}	0.0314
$\|g\|$	9.81	9.81	9.81
α_{TE}	3.43×10^{-3}	3.43×10^{-3}	3.43×10^{-3}
μ_f	1.511×10^{-5}	1.511×10^{-5}	1.511×10^{-5}
ρ_f	1.205	1.205	1.205
c_p^f	1005	1005	1005
κ_f	0.0257	0.0257	0.0257
ρ_s	2700	2700	2700
c_p^s	910	910	910
κ_s	237	237	237

3.2.6 Conclusions

Overall the levelset-XFEM approach appears to be an appealing method to tackle complex coupled systems such as the natural convection problem. Relevant physics are simply defined and material properties corresponding to different phases are incorporated exactly into the model, eliminating regions of intermediate material. It was shown that transient analysis is a critical component for analyzing and optimizing natural convection systems. The time scales of the natural convection systems modeled here were particularly problematic with the chosen setup however. A substantial number of time iterations was required that led to a single optimization step taking a particularly long time with no obvious solution using the current framework. Additionally, the levelset approach yields an optimization problem that can be difficult to appropriately regularize for effects such as feature size control.

3.3 Topology Optimization of Fluidic Cooling Devices with Constrained Structural Stress

3.3.1 Introduction

Since its development, topology optimization has been applied to a wide variety of single and multiphysics design problems. Levelset methods specifically have been used to solve structural, fluids, thermal, optical, electro-magnetic, electro-mechanical, and electro-thermo-mechanical problems ((van Dijk et al, 2013)). Levelset-XFEM approaches are particularly convenient for multiphysics problems due to the straight forward handling of any necessary interface conditions. Recently Coffin and Maute (2013), Maute et al (2011) and Makhija and Maute (2014) have thermal and coupled thermal-fluid design problems successfully using the levelset-XFEM.

Sigmund (2001a) and others have design problems that incorporate structural response to thermal loading for the purpose of actuation or damage limitation. The work of Sigmund (2001a) incorporates a Newton's Law of Cooling (NLC) boundary condition to simulate convective cooling of the device surface. This three-field (thermal-fluid-structural) coupled problem of structural response due to complex thermally induced stresses are of particular interest to the design of gas turbine blades. Gas turbine blades are subjected to large external temperatures that would result in structural damage over their life if not for cooling channels built into the blades themselves. Multidisciplinary design optimization has been performed by Talya et al (2002) on the turbine blade design problem. However the three-field problem appears to not have been tackled by topology optimization approaches, likely due to the challenging forward problem presented by fluid regime of interest.

In an effort to drive towards the challenging turbine blade design problem we begin with a simpler variation, the design of a heat sink/exchanger with limitations on the stress within the device. There appears to be no prior topology optimization of this coupled fluid-thermal-structural problem and so will present a new application of levelset-XFEM topology optimization.

3.3.2 Optimization Problem

We consider a two dimensional design problem shown in Figure 3.22. The design domain consists of a box containing two fluid inlets and two outlets. The domain will consist of one region of solid material Ω_s and two separate regions of fluid Ω_f. An external flow to the solid region will consist of a prescribed inlet flow velocity and cold temperature, while the internal flow will be prescribed with its own flow velocity profile and hot temperature. The design variables will be bounded so that there is a layer of solid guaranteed between the cold, outer fluid region and hot internal flow. We seek to minimize the temperature of the hot return fluid, exiting through outlet 4. The amount of solid material will be constrained as will the maximum stress in the solid material. The optimization problem is defined as:

$$\begin{aligned} min_{\mathbf{s}} \quad & \int T_f d\Gamma_4 \\ \text{s.t.} \quad & V_s - V_f c_v \leq 0, \\ & max_{\Omega_s}\left(\sigma_{vm}\right) - \sigma_{vm-max} \leq 0, \end{aligned} \tag{3.31}$$

where $\mathbf{s}$ is the vector of design variables, T_f is the fluid temperature, Γ_4 the hot fluid outlet, V_s the volume of solid material, V_f the volume of fluid region, c_v the limiting volume fraction, σ_{vm}

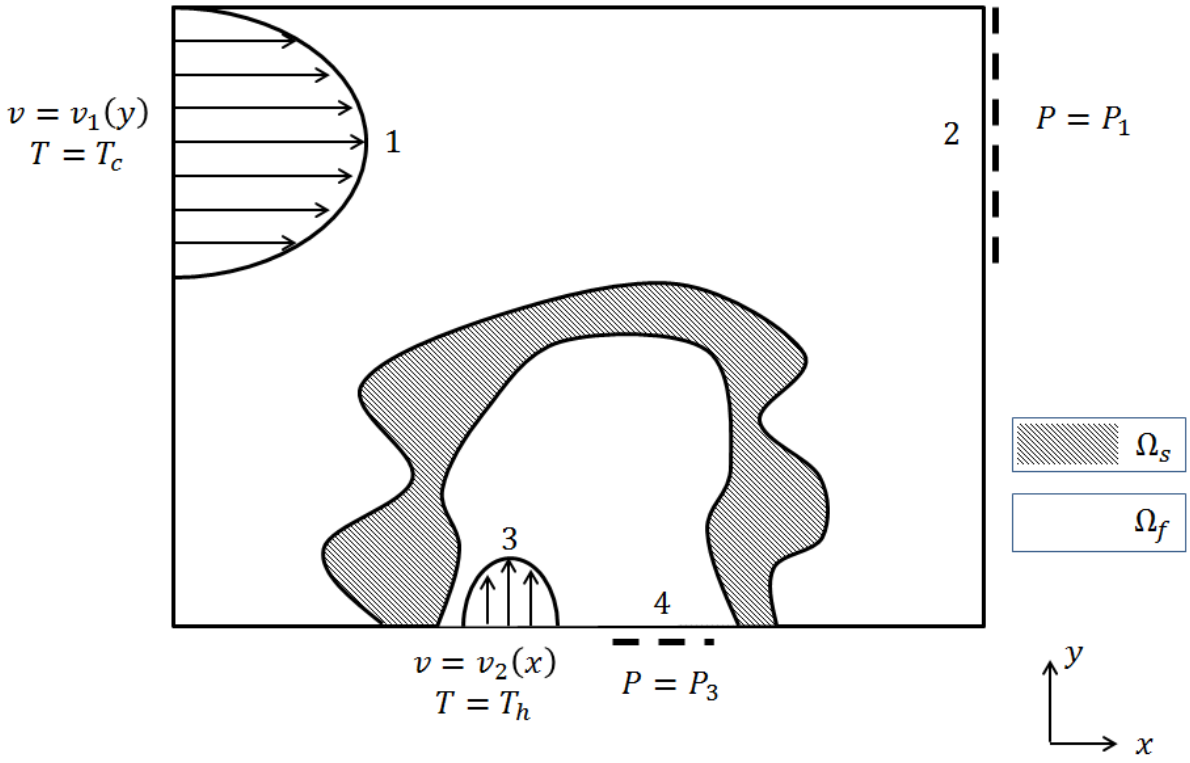

Figure 3.22: Cooling device optimization problem, cool fluid inlet (1), cool fluid outlet (2), hot fluid inlet (3), hot fluid outlet (4)

the elastic structural VonMises Stress and σ_{vm-max} the prescribed maximum allowable VonMises stress.

3.3.3 Governing Equations

The coupled problem will be governed by three equations, incompressible Navier-Stokes (fluid motion), advection-diffusion (temperature field) and linear elastic structures (elastic stress). The incompressible Navier-Stokes and advection-diffusion governing equations have been previously stated in Section 3.2.2 as Equations 3.24 and 3.25. Linear elasticity written in weak form and including isotropic thermal strain is:

$$R^{\sigma} = \int \delta\epsilon_{ij}\sigma_{ij}d\Omega_s - \int \delta u_i \sigma_{ij} n_j d\Gamma_{s,f} \tag{3.32}$$

where ϵ_{ij} is the linear strain, u_i the displacement, n_j the normal on the solid-fluid interface $\Gamma_{s,f}$ and the stress is:

$$\sigma_{ij} = C_{ijkl}\epsilon_{kl}^{elas} \tag{3.33}$$

where C_{ijkl} is the constitutive tensor and the elastic strain is computed as:

$$\epsilon_{ij}^{tot} = \epsilon_{ij}^{elas} + \epsilon_{ij}^{therm} \tag{3.34}$$

and the isotropic thermal strain is computed as:

$$\epsilon_{ij}^{therm} = \delta_{ij}\alpha\left(T_s - T_\infty\right) \tag{3.35}$$

where α is the coefficient of thermal expansion and T_∞ is the reference temperature. The total strain is computed as spatial derivatives of the interpolated displacements.

3.3.4 Levelset Geometry Definition and XFEM

An explicit levelset representation will be used to define the fluid and solid regions as shown previously in Equations 3.27 and 3.28. The XFEM will be applied to all fields as described in Section 3.2.3.

Chapter 4

Future Work and Conclusions

4.1 Future Work

4.1.1 Levelset Control

New Global Measure

The new global measure presented as Equation 2.6 in Section 2.2.2 should be applied to the topology optimization problem of Section 3.1.4, the thick, two-dimensional NLC convection problem. This will require reimplementation of the computation of the measure as well as implementation of sensitivity analysis for the measure. The measure should be reimplemented to replace the current point-by-point (intersection and node points) with a typical Gauss integration scheme over nearby elements. The sensitivity analysis will be broken into two components, a direct derivative ($\frac{\partial q}{\partial \mathbf{s}}$) and indirect component ($\frac{\partial q}{\partial \mathbf{u}}$). The direct derivative represents the partial derivative of the measure with respect to the design variables that influence the position of the interface and its normal direction. The indirect derivative will represent the partial derivative of the measure with respect to the state variables that are in turn influenced by the design variables. The additional derivative of the state variables with respect to the design variables will already be computed the code.

Once the measure is implemented and it and its derivatives are verified, it can be applied as a regularization to the two-dimensional, thick NLC design problem. The design problem has difficulties due to thin features in both material phases so two versions of the measure may need to be implemented. The formulation of the measure restricts it to regions in the direction of the interface normal, which could be reversed. The distance field would also need to be computed consistently in both phases. If the measure performs well with the NLC design problem an application to a typical structural design problem such as the so-called "force inverter" would be a convenient second test.

Robust Optimization

Robust optimization as presented by Sigmund (2009) and Jang et al (2012) present a shift from the typical forward analysis-optimizer interface. Effectively, a number of forward analyses much be completed to yield the objective value for the optimizer. This relation drives the scope of the work that will be required to implement this approach in FEMDOC. It will be necessary to provide additional functionality at the highest level of where the forward and sensitivity analysis are called by the optimization algorithm. A good understanding of the communication between the

optimization algorithm and the forward analysis to ensure that multiple forward and sensitivity analyses do not yield unexpected behavior. Depending on the current interface, the robust optimization implementation may be straight forward. Depending on time constraints of this work, efforts will be made to investigate different approaches to combining the forward and sensitivity analysis information for the best performance.

Regularization Comparison

A qualitative comparison of the user effort (at time of problem setup, to achieve well-formed designs) should be completed to provide future designers an understanding of the various approaches. A comparison of the computational time required for the various measures (both in forward analysis and sensitivity analysis) should also be compiled for a variety of problems and levels of mesh refinement. The combination of these two comparisons should yield future designers a better understanding of the total effort involved with these approaches. Particularly for large problems, most computationally costly measures may be more efficient as simpler measures may require a substantial amount of prior knowledge (acquired via test runs).

4.1.2 Applications

Three-dimensional Natural Convection

Three dimensional natural convection is currently on-going work. Handling of Lagrange multipliers on interfaces in three dimensions has been fixed so the values are consistently integrated across a particular interface. Previously rectangular interfaces would be broken into triangles and handled separately in an inconsistent fashion. A selection of test geometries should be run with a variety of interface scaling parameters and Lagrange multiplier options. These options include the type of interpolation of Lagrange multipliers over the interface (bi-linear or constant) as well as the integration domain for the compatibility term. The condition number of both the unconverged and converged systems should be compared to gain a better understanding of the most reliable set of parameters for the fluid interface conditions in three dimensional natural convection problems.

Design of Heat Exchanger with Mechanical Constraints

The heat exchanger design problem from Section 3.3 should be set up and run using the current framework. The current version of FEMDOC has all of the requisite machinery for this problem except for the so-called "coupled element" framework capable of coupling the three fields (incompressible Navier-Stokes, advection-diffusion and linear elasticity) with the incorporation of the XFEM. The three physics exist separately at current and also have a variety of currently functioning couplings, however the three-field case is non-existent.

In this work the mechanical stress field will be one-way coupled to the thermal field. The thermal field will also be one way coupled to the fluid field. That is that the fluid motion will drive the temperature field, which will in turn drive the mechanical stresses in the device. The final analysis component will be the incorporation of a maximum stress computation that will likely require a form of smoothed maximum function, such as the Kreisselmeier-Steinhauser function. As an initial step, the general topology optimization problem may also be replaced for the internal (hot) flow region with a parameter optimization problem using restricted channel shapes.

4.2 Conclusions

The convective cooling device design problem yields a challenging topology optimization problem that can exhibit a number of behaviors depending on the physical problem parameters chosen. The thick, two-dimensional NLC design problem has provided a good benchmark for evaluating the performance of simple regularization measures on a challenging problem. The problem also gives insight into the effects of the scaling of physics on the resultant designs. The addition of resolved fluid flow to the convection problem has shown the tradeoffs with this choice. The natural convection problem appears to be better behaved from a design geometry standpoint, however the solution to the forward analysis, particularly in three-dimensions can become difficult for certain material layouts. A three-physics design problem provides in an interesting opportunity to explore the associated difficulty of a complicated physical system in a topology optimization. This work will also explore a broad spectrum of levelset geometry control approaches on a consistent problem. Currently simple measures have been applied to design problems with mixed success. A more complicated measure has been evaluated for a set of design design geometries and appears promising to implement and apply design problems. The final approach, that of robust optimization is yet to be tested, however literature indicates promising behavior and the cost of implementation should be limited. In closing, the convective cooling design problem provides for a good test platform for evaluating different approaches to yielding well-formed design problems.

Bibliography

Alexandersen J, Andreasen C, Aage N, Lazarov B, Sigmund O (2013) Topology optimization for coupled convection problems. WCSMO 10

Alexandersen J, Aage N, Andreasen C, Sigmund O (2014) Topology optimisation for natural convection problems. International Journal for Numerical Methods in Fluids 00:1–23

Allaire G, Jouve F, Toader AM (2004) Structural optimization using sensitivity analysis and a level-set method. Journal of Computational Physics 194(1):363–393, DOI 10.1016/j.jcp.2003.09.032

Bahadur R, Bar-Cohen A (2005) Thermal design and optimization of natural convection polymer pin fin heat sinks. Components and Packaging Technologies, IEEE Transactions on 28(2):238–246

Belytschko T, Black T (1999) Elastic crack growth in finite elements with minimal remeshing. International Journal for Numerical Methods in Engineering 45

Bendsøe M (1989) Optimal shape design as a material distribution problem. Structural and Multidisciplinary Optimization 1(4):193–202, DOI 10.1007/BF01650949

Bendsøe M, Kikuchi N (1988) Generating optimal topologies in structural design using a homogenization method. Computer Methods in Applied Mechanics and Engineering 71(2):197–224

Bendsøe MP, Sigmund O (2003) Topology Optimization: Theory, Methods and Applications. Springer

Bruns T (2007) Topology optimization of convection-dominated, steady-state heat transfer problems. International Journal of Heat and Mass Transfer 50(15-16):2859 – 2873, DOI 10.1016/j.ijheatmasstransfer.2007.01.039

Burger M, Osher SJ (2005) A survey in mathematics for industry a survey on level set methods for inverse problems and optimal design. Euro Jnl of Applied Mathematics 16:263–301

Cengel YA, Klein S, Beckman W (1998) Heat transfer: a practical approach. WBC McGraw-Hill Boston

Chen S, Chen W (2011) A new level-set based approach to shape and topology optimization under geometric uncertainty. Structural and Multidisciplinary Optimization 44(1):1–18

Chen S, Wang M, Liu A (2008) Shape feature control in structural topology optimization. Computer-Aided Design 40(9):951–962

Coffin MD P, Maute K (2013) A method for optimizing the topology of cooling/heating devices using natural convection. WCSMO 10

Daux C, Moes N, Dolbow J, Sukumark N, Belytschko T (2000) Arbitrary branched and intersecting cracks with the extended finite element method. Int J Numer Meth Engng 48:1741–1760

van Dijk N, Langelaar M, van Keulen F (2012) Explicit level-set-based topology optimization using an exact heaviside function and consistent sensitivity analysis. International Journal for Numerical Methods in Engineering 91(1):67–97, DOI 10.1002/nme.4258

van Dijk N, Maute K, Langelaar M, Keulen F (2013) Level-set methods for structural topology optimization: a review. Structural and Multidisciplinary Optimization pp 1–36, DOI 10.1007/s00158-013-0912-y

Fries TP, Belytschko T (2006) The intrinsic xfem: A method for arbitrary discontinuities without additional unkowns. International Journal for Numerical Methods in Engineering 68:1358–1385, DOI 10.1002/nme.1761

Gerstenberger A, Wall WA (2008) An extended finite element method/Lagrange multiplier based approach for fluid-structure interaction. Computer Methods in Applied Mechanics and Engineering 197:1699–1714, DOI 10.1016/j.cma.2007.07.002

Gerstenberger A, Wall WA (2010) An embedded dirichlet formulation for 3d continua. International Journal for Numerical Methods in Engineering 82(5):537–563, DOI 10.1002/nme.2755

Guo X, Zhang W, Zhong W (2014) Explicit feature control in structural topology optimization via level set method. Computer Methods in Applied Mechanics and Engineering 272:354–378

Iga A, Nishiwaki S, Izui K, Yoshimura M (2009) Topology optimization for thermal conductors considering design-dependent effects, including heat conduction and convection. International Journal of Heat and Mass Transfer 52(11-12):2721–2732

Jang GW, Dijk NP, Keulen F (2012) Topology optimization of mems considering etching uncertainties using the level-set method. International Journal for Numerical Methods in Engineering 92(6):571–588

Jones M, Baerentzen JA, Sramek M (2006) 3d distance fields: A survey of techniques and applications. Visualization and Computer Graphics, IEEE Transactions on 12(4):581–599

Koga AA, Lopes ECC, Villa Nova HF, Lima CRd, Silva ECN (2013) Development of heat sink device by using topology optimization. International Journal of Heat and Mass Transfer 64:759–772

Kreissl S, Maute K (2011) Topology optimization for unsteady flow. International Journal for Numerical Methods in Engineering 87:1229–1253

Kreissl S, Maute K (2012) Levelset based fluid topology optimization using the extended finite element method. Structural and Multidisciplinary Optimization pp 1–16

Lang C, Makhija D, Doostan A, Maute K (2013) A simple and efficient preconditioning scheme for xfem with heaviside enrichments. Computational Mechancis

Lee K (2012) Topology optimization of convective cooling system designs. PhD thesis, The University of Michigan

Luo Z, Tong L, Wang MY, Wang S (2007) Shape and topology optimization of compliant mechanisms using a parameterization level set method. Journal of Computational Physics 227(1):680–705, DOI 10.1016/j.jcp.2007.08.011

Luo Z, Tong L, Luo J, Wei P, Wang M (2009) Design of piezoelectric actuators using a multiphase level set method of piecewise constants. Journal of Computational Physics 228(7):2643–2659

Makhija D, Maute K (2013) Numerical instabilities in level set topology optimization with the extended finite element method. Structural and Multidisciplinary Optimization

Makhija D, Maute K (2014) Level set topology optimization of scalar transport problems. Structural and Multidisciplinary Optimization DOI 10.1007/s00158-014-1142-7

Marck G, Nemer M, Harion JL (2013) Topology optimization of heat and mass transfer problems: laminar flow. Numerical Heat Transfer, Part B: Fundamentals 63(6):508–539

Matsumori T, Kondoh T, Kawamoto A, Nomura T (2013) Topology optimization for fluid–thermal interaction problems under constant input power. Structural and Multidisciplinary Optimization 47(4):571–581

Maute K, Kreissl S, Makhija D, Yang R (2011) Topology optimization of heat conduction in nano-composites. In: 9$^{\text{th}}$ World Congress on Structural and Multidisciplinary Optimization, Shizuoka, Japan

McConnell C, Pingen G (2012) Multi-layer, pseudo 3d thermal topology optimization of heat sinks. In: ASME 2012 International Mechanical Engineering Congress and Exposition, American Society of Mechanical Engineers, pp 2381–2392

Moes N, Dolbow J, Belytschko T (1999) A finite element method for crack growth without remeshing. International Journal for Numerical Methods in Engineering 46

Mohamadian M, Shojaee S (2011) Binary level set method for structural topology optimization with mbo type of projection. International Journal for Numerical Methods in Engineering xx:xx–xx

Moon H, Kim C, Wang S (2004) Reliability-based topology optimization of thermal systems considering convection heat transfer. In: Tenth AIAA/ISSMO multidisciplinary analysis and optimization conference. Albany, New York

Morrison AT (1992) Optimization of heat sink fin geometries for heat sinks in natural convection. In: Thermal Phenomena in Electronic Systems, 1992. I-THERM III, InterSociety Conference on, IEEE, pp 145–148

Osher S, Fedkiw R (2002) Level set methods and dynamic implicit surfaces, vol 153. Springer

Pingen G, Meyer D (2009) Topology optimization for thermal transport. In: ASME 2009 Fluids Engineering Division Summer Meeting, American Society of Mechanical Engineers, pp 2237–2243

Pingen G, Waidmann M, Evgrafov A, Maute K (2010) A parametric level-set approach for topology optimization of flow domains. Structural and Multidisciplinary Optimization 41(1):117–131, DOI 10.1007/s00158-009-0405-1

Rozvany G, Zhou M, Birker T (1992) Generalized shape optimization without homogenization. Structural and Multidisciplinary Optimization 4(3):250–252

de Ruiter M, van Keulen F (2001) Topology optimization using the topology description function approach. In: Cheng G, Gu Y, Liu S, Wang Y (eds) 4$^{\text{th}}$ World Congress on Structural and Multidisciplinary Optimization, Dailan, China

Seo JH (2009) Optimal design of material microstructure for convective heat transfer in a solid-fluid mixture. PhD thesis, University of Michigan at Ann Arbor

Sigmund O (2001a) Design of multiphysics actuators using topology optimization – Part I: One–material structures. Computer Methods in Applied Mechanics and Engineering 190(49–50):6577–6604

Sigmund O (2001b) Design of multiphysics actuators using topology optimization - part II: Two-material structures. Computer Methods in Applied Mechanics and Engineering 190(49-50):6605–6627

Sigmund O (2009) Manufacturing tolerant topology optimization. Acta Mechanica Sinica/Lixue Xuebao 25(2):227–239

Sigmund O, Maute K (2013) Topology optimization approaches: A comparative review. Structural and Multidisciplinary Optimization

Stenberg R (1995) On some techniques for approximating boundary conditions in the finite element method. Journal of Computational and Applied Mathematics 63(1-3):139 – 148, DOI 10.1016/0377-0427(95)00057-7

Svanberg K (1995) A globally convergent version of MMA without linesearch. In: Proceedings of the First World Congress of Structural and Multidisciplinary Optimization, 28 May - 2 June 1995, Goslar, Germany, pp 9–16

Talya S, Chattopadhyay A, Rajadas J (2002) Multidisciplinary design optimization procedure for improved design of a cooled gas turbine blade. Engineering Optimization 34(2):175–194

Tezduyar TE (1992) Stabilized finite element formulations for incompressible flow computations. Advances in Applied Mechanics 28:1–44

Tucker P (1998) Assessment of geometric multilevel convergence robustness and a wall distance method for flows with multiple internal boundaries. Applied Mathematical Modelling 22(4):293–311

Tucker P (2003) Differential equation-based wall distance computation for des and rans. Journal of computational physics 190(1):229–248

Wang M, Wang X (2004) PDE-driven level sets, shape sensitivity and curvature flow for structural topology optimization. Computer Modeling in Engineering & Sciences 6(4):373–395

Wang M, Zhou S (2004) Phase field: a variational method for structural topology optimization. Computer Modeling in Engineering & Sciences 6(6):547–566

Wang S, Wang M (2006) Radial basis functions and level set method for structural topology optimization. International journal for numerical methods in engineering 65(12):2060–2090

Yamada T, Izui K, Nishiwaki S (2011) A level set-based topology optimization method for maximizing thermal diffusivity in problems including design-dependent effects. Journal of Mechanical Design 133:031,011–1–031,011–9

Yin L, Ananthasuresh G (2002) A novel topology design scheme for the multi-physics problems of electro-thermally actuated compliant micromechanisms. Sensors and Actuators A: Physical 97:599–609

Yoon G, Kim Y (2005) The element connectivity parameterization formulation for the topology design optimization of multiphysics systems. International journal for numerical methods in engineering 64(12):1649–1677

Yoon GH (2010) Topological design of heat dissipating structure with forced convective heat transfer. Journal of Mechanical Science and Technology 24:1225–1233

Zhou M, Rozvany GIN (1991) The COC algorithm, part II: Topological, geometrical and generalized shape optimization. Computer Methods in Applied Mechanics and Engineering 89(1-3):309–336